
Fair Coresets via Optimal Transport

Zikai Xiong^{1*} Niccolò Dalmaso² Shubham Sharma² Freddy Lecue²
Daniele Magazzeni² Vamsi K. Potluru² Tucker Balch² Manuela Veloso²

Abstract

Data distillation and coresets have emerged as popular approaches to generate a smaller representative set of samples for downstream learning tasks to handle large-scale datasets. At the same time, machine learning is being increasingly applied to decision-making processes at a societal level, making it imperative for modelers to address inherent biases towards subgroups present in the data. Current approaches create fair synthetic representative samples by optimizing local properties relative to the original samples, but their effect on downstream learning processes has yet to be explored. In this work, we present fair Wasserstein coresets (FWC), a novel coreset approach which generates fair synthetic representative samples along with sample-level weights to be used in downstream learning tasks. FWC minimizes the Wasserstein distance between the original dataset and the weighted synthetic samples while enforcing demographic parity. We show that an unconstrained version of FWC is equivalent to Lloyd’s algorithm for k-medians and k-means clustering. Experiments conducted on both synthetic and real datasets show that FWC: (i) achieves a competitive fairness-performance tradeoff in downstream models compared to existing approaches, (ii) improves downstream fairness when added to the existing training data and (iii) can be used to reduce biases in predictions from large language models (GPT-3.5 and GPT-4).

1. Introduction

In the last decade, the rapid pace of technological advancement has provided the ability of collecting, storing and processing massive amounts of data from multiple sources

^{*}Work done while at J.P.Morgan AI Research ¹Massachusetts Institute of Technology ²J.P.Morgan AI Research, New York. Correspondence to: Niccolò Dalmaso <niccolo.dalmaso@jpmchase.com>.

(Sapiroglu & Sinanc, 2013). As the volume of data continues to surge, it often surpasses both the available computational resources as well as the capacity of machine learning algorithms. In response to this limitation, dataset distillation approaches aim to reduce the amount of data by creating a smaller, yet representative, set of samples; see Yu et al. (2023); Lei & Tao (2024) for comprehensive reviews on the topic. Among those approaches, coresets provide a weighted subset of the original data that achieve similar performance to the original dataset in (usually) a specific machine learning task, such as clustering (Har-Peled & Mazumdar, 2004; Feldman, 2020), Bayesian inference (Campbell & Broderick, 2018), online learning (Borsos et al., 2020) and classification (Coleman et al., 2020), among others.

In tandem with these developments, the adoption of machine learning techniques has seen a surge in multiple decision-making processes that affect society at large (Sloane et al., 2022; Zhang et al., 2022). This proliferation of machine learning applications has highlighted the need to mitigate inherent biases in the data, as these biases can significantly impact the equity of machine learning models and their decisions (Chouldechova, 2017). Among many definitions of algorithmic fairness, demographic parity is one of the most prominently used metric (Hort et al., 2023), enforcing the distribution of an outcome of a machine learning model to not differ dramatically across different subgroups in the data.

Current methodologies for generating a smaller set of fair representative samples focus on the local characteristics of these samples with respect to the original dataset. For instance, Chierichetti et al. (2017); Huang et al. (2019); Backurs et al. (2019); Ghadiri et al. (2021) enforce representative points obtained by clustering so that each cluster includes the same proportion of points from each subgroup in the original dataset. In another line of work, Jung et al. (2019); Mahabadi & Vakilian (2020); Negahbani & Chakrabarty (2021); Vakilian & Yalciner (2022); Chhaya et al. (2022) create representative points by ensuring that points in the original dataset each have at least one representative point within a given distance in the feature space. While these methods can successfully reduce clustering cost and ensure a more evenly spread-out distribution of representative points in the feature space, it is unclear whether such representative

samples can positively affect performance or discrimination reduction in downstream learning processes. As the induced distribution of the representative points might be far away from the original dataset distribution, downstream machine learning algorithm might lose significant performance without necessarily reducing biases in the original data (as we also demonstrated empirically in our experiments).

Contributions In this work, we introduce **Fair Wasserstein Coresets (FWC)**, a novel coreset approach that not only generates synthetic representative samples but also assigns sample-level weights to be used in downstream learning tasks. FWC generates synthetic samples by minimizing the Wasserstein distance between the distribution of the original datasets and that of the weighted synthetic samples, while simultaneously enforcing an empirical version of demographic parity. The Wasserstein distance is particularly useful when generating coresets, as downstream model performance is tied to the Wasserstein distance’s dual formulation (Section 2). Our contributions are as follows:

1. we show how the FWC optimization problem can be reduced to a nested minimization problem in which fairness constraints are equivalent to linear constraints (Section 3);
2. we propose a majority minimization algorithm to solve the reformulated problem (Section 4). Additionally, in absence of fairness constraints, we show our algorithm reduces to an equivalent version of Lloyd’s algorithm for k-means and k-medians clustering, extending its applicability beyond fairness applications (Section 4.4);
3. we empirically validate the effectiveness of FWC by providing experiments on both synthetic and real-world datasets (Section 5). When compared against current approaches, FWC achieves competitive performance, even when we enhance the fairness of existing approaches using existing fair pre-processing techniques. In addition, we show FWC can correct biases in downstream model biases when added to the training data (via data augmentation), as well as in large language models (GPT-3.5 (OpenAI, 2022) and GPT-4 (Achiam et al., 2023)) when passing coresets as examples to the LLM.

Finally, we refer the reader to the appendixs for more details on the optimization problem (Section A), theoretical proofs of lemmas and theorems (Section B) and experiment details (Section C).

2. Background

Notation We indicate the original dataset samples $\{Z_i\}_{i=1}^n$, with $Z_i = (D_i, X_i, Y_i) \in \mathcal{Z} = (\mathcal{D} \times \mathcal{X} \times \mathcal{Y})$,

where X indicates the non-sensitive features, D indicates one or more protected attributes such as ethnicity or gender, and Y is a decision outcome. In this work, we assume D and Y to be discrete features, i.e., to have a finite number of levels so that $|\mathcal{D}| \ll n$ and $|\mathcal{Y}| \ll n$. For example, Y might indicate a credit card approval decision based on credit history X , with D denoting sensitive demographic information. Given a set of weights $\{\theta\}_{i=1}^n$, define $p_{Z;\theta}$ the weighted distribution of a dataset $\{Z_i\}_{i=1}^n$ as

$$p_{Z;\theta} \stackrel{\text{def.}}{=} \frac{1}{n} \sum_{i=1}^n \theta_i \delta_{Z_i},$$

where δ_x indicates the Dirac delta distribution, i.e., the unit mass distribution at point $x \in \mathcal{X}$. Using this notation, we can express the empirical distribution of the original dataset by setting $\theta_i = e_i = 1$ for any i , i.e., $p_{Z;e} = \frac{1}{n} \sum_{i=1}^n e_i \delta_{Z_i}$. For a matrix A , A^\top denotes its transpose. For two vectors (or matrices) $\langle u, v \rangle \stackrel{\text{def.}}{=} \sum_i u_i v_i$ is the canonical inner product (the Frobenius dot-product for matrices). We define $\mathbf{1}_m \stackrel{\text{def.}}{=} (1, \dots, 1) \in \mathbb{R}_+^m$. We use $\mathbb{P}(\mathcal{X})$ to indicate the set of probability distributions over a metric space \mathcal{X} .

Measure Coreset Let \mathcal{F} be the hypothesis set for a learning problem, with functions $f \in \mathcal{F}$ mapping from \mathcal{Z} to \mathbb{R} . We follow the definition in (Claici et al., 2018) and say that a weighted dataset $\{\widehat{Z}_i = (\widehat{X}_i, \widehat{D}_i, \widehat{Y}_i), \theta_i\}_{i=1}^m$ is a δ -coreset if

$$\sup_{f \in \mathcal{F}} \left| \text{cost}(Z, w, f) - \text{cost}(\widehat{Z}, \theta, f) \right| \leq \delta,$$

$$\text{where } \text{cost}(Z, w, f) \stackrel{\text{def.}}{=} \sum_{i=1}^n w_i f(Z_i). \quad (1)$$

In this definition, finding a δ -coreset corresponds to obtaining a weighted dataset $\{\widehat{Z}_i, \theta_i\}_{i=1}^m$ such that $m \ll n$ and with a small δ . This definition of δ -coreset highlights the importance of preserving the performance of downstream learning models on the original dataset $\{Z_i\}_{i=1}^n$.

Wasserstein Distance Given two probability distributions p_1 and p_2 over a metric space \mathcal{X} , the Wasserstein distance, or optimal transport metric, quantifies the distance between the two distributions as solution of the following linear program (LP):

$$\mathcal{W}_c(p_1, p_2) \stackrel{\text{def.}}{=} \min_{\pi \in \Pi(p_1, p_2)} \int_{\mathcal{X} \times \mathcal{X}} c(x_1, x_2) d\pi(x_1, x_2), \quad (2)$$

with $\Pi(p_1, p_2)$ indicating the set of all joint probability distributions over the product space $\mathcal{X} \times \mathcal{X}$ with marginals

equal to (p_1, p_2) (Kantorovitch, 1958). The operator $c(x, y)$ represents the “cost” of moving probability mass from x and y , and reduces to a matrix C if the underlying metric space \mathcal{X} is discrete. Given a metric space \mathcal{X} endowed with a metric $d_{\mathcal{X}}$, the usual choice is to set $c(x, y) = d_{\mathcal{X}}(x, y)^p$ for $p \geq 1$, which corresponds to the p -Wasserstein distance between probability measures $\mathcal{W}_c^{1/p}$ in Equation (2).

The Wasserstein distance $\mathcal{W}_c(p_1, p_2)$ can also be used to bound the deviation of functions applied to samples from p_1 and p_2 , respectively. Define the following deviation:

$$d(p_1, p_2) \stackrel{\text{def.}}{=} \sup_{f \in \mathcal{F}} |\mathbb{E}_{z \sim p_1} f(z) - \mathbb{E}_{z \sim p_2} f(z)|,$$

where \mathcal{F} is a class of functions f . When \mathcal{F} is the class of Lipschitz-continuous functions with Lipschitz constant of 1, the deviation $d(p_1, p_2)$ is equal to 1-Wasserstein distance $\mathcal{W}^1(p_1, p_2)$ (Santambrogio, 2015; Villani et al., 2009). Similarly, if \mathcal{F} is the class of functions with unitary norm over the Sobolev space, the 2-Wasserstein distance upper bounds the deviation above, i.e., $d(p_1, p_2) \leq \mathcal{W}^{1/2}(p_1, p_2)$. This fact provides a theoretical intuition for evaluating the quality of a coreset. The closer the Wasserstein distance between the empirical distribution formed by the coreset and the one formed by the original dataset, then the smaller the left-hand side of Equation (1) could be. Finally, Wasserstein distance and optimal transport have been extensively applied in algorithmic fairness, although not specifically for coresets; see, e.g., Gordaliza et al. (2019); Black et al. (2020); Silvia et al. (2020) and references therein.

Demographic parity Also known as statistical parity, demographic parity (DP) imposes the decision outcome and protected attributes to be independent (Dwork et al., 2012). Using a credit card approval decision example, demographic parity enforces an automatic decision process to approve similar proportion of applicants across different race demographics. DP is one of the most extensively analyzed fairness criterion; we refer the reader to Hort et al. (2023) for a review. In this work, we use the demographic parity definition by Calmon et al. (2017), which enforces the ratio between the conditional distribution of the decision outcome across each subgroups $p(y|D = d)$ and the marginal distribution of the decision outcome $p(y)$ to be close to 1 in a given dataset. We refer to the “empirical version” of demographic parity to indicate that the conditional and marginal distributions are quantities estimated from the data.

3. FWC: Fair Wasserstein Coresets

Given a dataset $\{Z_i\}_{i=1}^n$, our goal is to find a set of samples $\{\hat{Z}_j\}_{j=1}^m$ and weights $\{\theta_j\}_{j=1}^m$ such that $m \ll n$ and that the Wasserstein distance between $p_{Z;e}$ and $p_{\hat{Z};\theta}$, $\mathcal{W}_c(p_{\hat{Z};\theta}, p_{Z;e})$, is as small as possible. In addition, we use

the fairness constraints proposed by Calmon et al. (2017) and Xiong et al. (2023) to control the demographic parity violation for the $p_{\hat{Z};\theta}$ distribution. In practice, this reduces to requiring the conditional distribution under the weights $\{\theta_i\}_{i \in [n]}$ to be close to a target distribution p_{Y_T} across all possible values of the protected attributes D ,

$$J\left(p_{\hat{Z};\theta}(\hat{Y} = y|\hat{D} = d), p_{Y_T}(y)\right) \leq \epsilon, \forall d \in \mathcal{D}, y \in \mathcal{Y}, \quad (3)$$

where ϵ is a parameter that determines the maximum fairness violation, and $J(\cdot, \cdot)$ denotes a symmetric probability ratio between distributions defined in the following way:

$$J(p, q) = \max\left\{\frac{p}{q} - 1, \frac{q}{p} - 1\right\}. \quad (4)$$

For simplicity, we will use $p_{\hat{Z};\theta}(y|d)$ to indicate the conditional distribution $p_{\hat{Z};\theta}(\hat{Y} = y|\hat{D} = d)$.

Using the notation above, our goal can then be formulated as the following optimization problem:

$$\begin{aligned} \min_{\theta \in \Delta_m, \hat{Z} \in \mathcal{Z}^m} \quad & \mathcal{W}_c(p_{\hat{Z};\theta}, p_{Z;e}) \\ \text{s.t.} \quad & J\left(p_{\hat{Z};\theta}(y|d), p_{Y_T}(y)\right) \leq \epsilon, \forall d \in \mathcal{D}, y \in \mathcal{Y}, \end{aligned} \quad (5)$$

where Δ_m indicates the set of valid weights $\{\theta \in \mathbb{R}_+^m : \sum_{i=1}^m \theta_i = m\}$. Note that the optimization problem in (5) shares some similarities with the optimization problem in Xiong et al. (2023, Equation 3) in using the Wasserstein distance as a distance metric between distributions and using (4) to enforce demographic parity. However, Xiong et al. (2023) only provide sample-level integer weights for the original dataset and do not generate any new samples, while our approach provides a separate set of samples $\{\hat{Z}_j\}_{j=1}^m$ with associated real-valued weights $\{\theta_j\}_{j=1}^m$, with $m \ll n$.

We now take the following steps to solve the optimization problem in (5): (i) we reduce the dimensionality of the feasible set by fixing \hat{Y} and \hat{D} a priori, (ii) we formulate the fairness constraints as linear constraints, (iii) we add artificial variables to express the objective function and (iv) we simplify the optimization problem to minimizing a continuous non-convex function of the $\{X_j\}_{j=1}^m$. Finally, we propose a majority minimization method to solve the optimization problem, which we analyze in Section 4.

Step 1. Reduce the optimization problem feasible set

As in practice all possible Y_i and D_i are known a priori, and there are only a limited number of them, we can avoid optimizing over them and instead manually set the proportion of each combination of \hat{Y} and \hat{D} . This reduces the optimization problem feasible set only over Δ_m and \mathcal{X}^m . The following lemma shows that this in fact does not affect the optimization problem:

Lemma 3.1. *For any $m > 0$, the best fair Wasserstein coreset formed by m data points $\{\widehat{Z}_i : i \in [m]\}$ is no better than the best fair Wasserstein coreset formed by $m|\mathcal{D}||\mathcal{Y}$ data points $\{(d, X_i, y)_i : i \in [m], d \in \mathcal{D}, y \in \mathcal{Y}\}$.*

Hence, we simply set the proportions of $\{(\widehat{D}_i, \widehat{Y}_i)_{i \in [m]}\}$ in the coresets to be similar to their respective proportions in the original dataset. The optimization problem then reduces to finding the features in the coreset $\{\widehat{X}_j\}_{j=1}^m$ and corresponding weights $\{\theta_j\}_{j=1}^m$ such that:

$$\begin{aligned} \min_{\theta \in \Delta_m, \widehat{X} \in \mathcal{X}^m} \mathcal{W}_c(p_{\widehat{Z}; \theta}, p_{Z; \epsilon}) \\ \text{s. t. } J(p_{\widehat{Z}; \theta}(y|d), p_{Y_T}(y)) \leq \epsilon, \forall d \in \mathcal{D}, y \in \mathcal{Y}. \end{aligned} \quad (6)$$

Step 2. Equivalent linear constraints Following Xiong et al. (2023), the fairness constraint in Equation (3) can be expressed as a linear constraint. First, note that the conditional probability $p_{\widehat{Z}; \theta}(y|d)$ can be written in the following form:

$$p_{\widehat{Z}; \theta}(y|d) = \frac{\sum_{i \in [m]: \widehat{D}_i = d, \widehat{Y}_i = y} \theta_i}{\sum_{i \in [m]: \widehat{D}_i = d} \theta_i}.$$

Given the definition of demographic parity in Equation (4), the ratio reduces to the following set of equations for all $d \in \mathcal{D}, y \in \mathcal{Y}$:

$$\begin{aligned} \sum_{i \in [m]: \widehat{D}_i = d, \widehat{Y}_i = y} \theta_i &\leq (1 + \epsilon) \cdot p_{Y_T}(y) \cdot \sum_{i \in [m]: \widehat{D}_i = d} \theta_i, \\ \sum_{i \in [m]: \widehat{D}_i = d, \widehat{Y}_i = y} \theta_i &\geq \frac{1}{1 + \epsilon} \cdot p_{Y_T}(y) \cdot \sum_{i \in [m]: \widehat{D}_i = d} \theta_i. \end{aligned} \quad (7)$$

This implies that we can reformulate the fairness constraint as $2|\mathcal{Y}||\mathcal{D}|$ linear constraints on the weights θ . We can express these by using a $2|\mathcal{Y}||\mathcal{D}|$ -row matrix A as $A\theta \geq 0$.

Step 3. Reformulate the objective function by introducing artificial variables When keeping the samples \widehat{X} fixed, we can follow Peyré et al. (2019) to derive an equivalent formulation of the Wasserstein distance in the objective as a linear program with mn variables. By indicating the transportation cost matrix $C(\widehat{X})$, we define its components as follows,

$$C(\widehat{X})_{ij} \stackrel{\text{def.}}{=} c(Z_i, \widehat{Z}_j), \text{ for } i \in [n], j \in [m].$$

Note that $C(\widehat{X})$ is a convex function of \widehat{X} when, e.g., using any L^p norm to define the transportation cost. Therefore,

now the problem (6) is equivalent to

$$\begin{aligned} \min_{\widehat{X} \in \mathcal{X}^m, \theta \in \Delta_m, P \in \mathbb{R}^{n \times m}} \langle C(\widehat{X}), P \rangle \\ \text{s. t. } P\mathbf{1}_m = \frac{1}{n} \cdot \mathbf{1}_n, P^\top \mathbf{1}_n = \frac{1}{m} \cdot \theta, P \geq 0, A\theta \geq 0. \end{aligned} \quad (8)$$

Step 4. Reduce to an optimization problem of \widehat{X} Consider any feasible (\widehat{X}, θ, P) of problem (8). It holds that:

- $\theta = m \cdot P^\top \mathbf{1}_n$;
- Since $\frac{1}{n} \cdot \mathbf{1}_n^\top \mathbf{1}_n = 1$, if $P\mathbf{1}_m = \frac{1}{n} \cdot \mathbf{1}_n$ then $\theta^\top \mathbf{1}_m = m$.

Hence, problem (8) is then simplified by replacing variables θ with $m \cdot P^\top \mathbf{1}_n$.

$$\begin{aligned} \min_{\widehat{X} \in \mathcal{X}^m, P \in \mathbb{R}^{n \times m}} \langle C(\widehat{X}), P \rangle \\ \text{s. t. } P\mathbf{1}_m = \frac{1}{n} \cdot \mathbf{1}_n, P \geq 0, AP^\top \mathbf{1}_n \geq 0. \end{aligned} \quad (9)$$

Let $F(C)$, as a function F of C , denote the optimal objective value of the following optimization problem

$$\begin{aligned} \min_{P \in \mathbb{R}^{n \times m}} \langle C, P \rangle \\ \text{s. t. } P\mathbf{1}_m = \frac{1}{n} \cdot \mathbf{1}_n, P \geq 0, AP^\top \mathbf{1}_n \geq 0 \end{aligned} \quad (10)$$

and then problem (9) is equivalent to

$$\min_{\widehat{X} \in \mathcal{X}^m} F(C(\widehat{X})). \quad (11)$$

In (11) the objective is continuous but nonconvex with respect to \widehat{X} . Once the optimal \widehat{X}^* is solved, then the optimal P^* of the problem (9) is obtained by solving problem (10) with C replaced with $C(\widehat{X}^*)$. Finally, the optimal θ^* follows by the equation $\theta^* = m \cdot (P^*)^\top \mathbf{1}_n$. We now provide a majority minimization algorithm for solving problem (11).

4. Majority Minimization for Solving the Reformulated Problem

Majority minimization aims at solving nonconvex optimization problems, and refers to the process of defining a convex surrogate function that upper bounds the nonconvex objective function, so that optimizing the surrogate function improves the objective function (Ortega & Rheinboldt, 2000; Lange, 2016). As the algorithm proceeds, the surrogate function also updates accordingly, which ensures the value of the original objective function keeps decreasing. Following this framework, we define the surrogate function $g(\cdot; \widehat{X}^k)$ as follows for the k -th iterate $\widehat{X}^k \in \mathcal{X}^m$:

$$g(\widehat{X}; \widehat{X}^k) \stackrel{\text{def.}}{=} \langle C(\widehat{X}), P_k^* \rangle, \quad (12)$$

Algorithm 1 Majority Minimization for Solving (11)

```

1: Initial feature vectors  $\widehat{X}^k$  and  $k = 0$ 
2: while True do
3:    $C \leftarrow C(\widehat{X}^k)$ ;  $\triangleright$  update the cost matrix  $C$ 
4:    $P_k^* \leftarrow$  optimal solution of problem (10);  $\triangleright$  update the ingredient of the surrogate function
5:    $\widehat{X}^{k+1} \leftarrow \arg \min_{\widehat{X} \in \mathcal{X}^m} g(\widehat{X}; \widehat{X}^k)$ ;  $\triangleright$  update feature vectors by minimizing the surrogate function
6:   if  $g(\widehat{X}^{k+1}; \widehat{X}^k) = g(\widehat{X}^k; \widehat{X}^k)$  then
7:      $\theta_k^* \leftarrow m \cdot (P_k^*)^\top \mathbf{1}_n$ ;  $\triangleright$  if algorithm has converged, compute optimal weights
8:     return  $\widehat{X}^k, \theta_k^*$ ;  $\triangleright$  return coresets and sample-level weights
9:   end if
10:   $k \leftarrow k + 1$ ;
11: end while
    
```

in which P_k^* is the minimizer of problem (10) with the cost $C = C(\widehat{X}^k)$ ¹.

With this surrogate function, Algorithm 1 summarizes the overall algorithm to minimize problem (11). In each iteration of Algorithm 1, line 3 is straightforward since it only involves computing the new cost matrix using the new feature vectors \widehat{X}^k . We separately discuss how to solve the optimization problems in lines 4 and 5 below.

4.1. Updating the surrogate function (line 4)

To update the surrogate function, we need to solve problem (10), which is a huge-scale linear program with $O(n)$ constraints and $O(mn)$ nonnegative variables. Given the problem size becomes computationally prohibitive for large values of n and m , we propose to use a variant of FairWASP, a fast algorithm proposed by Xiong et al. (2023) to find the solution of (10) via applying the cutting plane methods on the Lagrangian dual problems with reduced dimension. More specifically, we adapt FairWASP for cases where $m \neq n$, as opposed to the scenario where $m = n$, which was tackled by Xiong et al. (2023). We choose FairWASP over established commercial solvers due to its computational complexity being lower than other state of the art approaches such as interior-point or simplex method (Xiong et al. 2023, Section 5). We include the details of the formulation of the Lagrangian dual problem and the details of the cutting plane methods in Appendix A.

4.2. Updating feature vectors (line 5)

To update the feature vectors, we need to obtain the minimizer of the surrogate function $g(\widehat{X}; \widehat{X}^k)$, i.e.,

$$\min_{\widehat{X} \in \mathcal{X}^m} g(\widehat{X}; \widehat{X}^k). \quad (13)$$

¹We show this surrogate function is adequate, i.e., is convex and an upper bound of the original objective function, in Section 4.3.

The above can be written as the following problem:

$$\min_{\widehat{X}_i \in \mathcal{X}: i \in [m]} \sum_{i \in [m]} \sum_{j \in [n]} c(Z_i, \widehat{Z}_j) P_{ij} \quad (14)$$

for $P = P_k^*$, in which each component of P is nonnegative and $\widehat{Z}_j = (\widehat{d}_j, \widehat{X}_j, \widehat{y}_j)$, for the known fixed \widehat{d}_i and \widehat{y}_i . Furthermore, the matrix P is sparse, containing at most n non-zeros (as when updating P_k^* for problem (10), see Appendix A). Moreover, problem (14) can be separated into the following m subproblems,

$$\min_{\widehat{X}_i \in \mathcal{X}} \sum_{i \in [n]} c(Z_i, \widehat{Z}_j) P_{ij}, \text{ for } j \in [m]. \quad (15)$$

Each subproblem computes the weighted centroid of $\{Z_i : i \in [n], P_{ij} > 0\}$ under the distance function c . Therefore, (13) is suitable for parallel and distributed computing. Additionally, since the cost matrix $C(\widehat{X})$ is a convex function of \widehat{X} , each subproblem is a convex problem so gradient-based methods could converge to global minimizers. Furthermore, under some particular conditions, solving these small subproblems can be computationally cheap:

1. If \mathcal{X} is convex and $c(Z, \widehat{Z}) \stackrel{\text{def.}}{=} \|Z - \widehat{Z}\|_2^2$, then the minimizer of (15) is the weighted average $\sum_{i \in [n]} P_{ij} X_i / \sum_{i \in [n]} P_{ij}$.
2. If \mathcal{X} is convex and $c(Z, \widehat{Z}) \stackrel{\text{def.}}{=} \|Z - \widehat{Z}\|_1$, then the minimizer of (15) requires sorting the costs coordinate-wisely and finding the median.
3. If creating new feature vectors is not permitted and $\mathcal{X} = \{X_i : i \in [n]\}$, solving (15) requires finding the smallest $\sum_{i \in [n]} c(Z_i, (\widehat{d}_j, X, \widehat{y}_j)) P_{ij}$ for X within the finite set \mathcal{X} . The matrix P is highly sparse so this operation is not computationally expensive.

As we have shown Algorithm 1 is feasible and (computationally) inexpensive, we now analyze its convergence behavior in the next section.

4.3. Convergence guarantees

First, we show that the surrogate function $g(\widehat{X}; \widehat{X}^k)$ is indeed convex and an upper bound of $F(C(\widehat{X}))$.

Lemma 4.1. *The function $g(\widehat{X}; \widehat{X}^k)$ is convex function of \widehat{X} and a valid upper bound, i.e., $g(\widehat{X}; \widehat{X}^k) \geq F(C(\widehat{X}))$. This inequality holds at equality when $\widehat{X} = \widehat{X}^k$.*

Given the above, Theorem 4.2 shows the optimization problem in (11) converges to a first-order stationary point.

Theorem 4.2. *The objective value is monotonically decreasing, i.e., $F(C(\widehat{X}^{k+1})) \leq F(C(\widehat{X}^k))$ for any $k \geq 0$. And once the algorithm stops and $C(\widehat{X}^k)$ is smooth at \widehat{X}^k , then \widehat{X}^k is a first-order stationary point of (11).*

Finally, when the minimizer of the problem (13) is unique, we show Algorithm 1 has finite termination.

Theorem 4.3. *When the minimizer of (13) is unique, Algorithm 1 terminates within finite iterations.*

Note that because $g(\widehat{X}; \widehat{X}^k) = \langle C(\widehat{X}), P_k^* \rangle$, the minimizer is unique whenever the cost matrix $C(\cdot)$ is strongly convex. We refer the reader to Appendix B for the proofs of this subsection.

4.4. An alternative view: Generalized clustering algorithm

When the fairness constraints are absent, the problem (10) reduces to:

$$\begin{aligned} \min_{P \in \mathbb{R}^{n \times m}} \quad & \langle C, P \rangle \\ \text{s.t.} \quad & P \mathbf{1}_m = \frac{1}{n} \cdot \mathbf{1}_n, P \geq \mathbf{0}_{n \times m}. \end{aligned} \quad (16)$$

The minimizer P^* of (16) can be written in closed form. For each $i \in [n]$, let $C_{ij_i^*}$ denote a smallest component on the i -th row of C . Then the components of a minimizer P^*

$$\text{can be written as } P_{ij}^* = \begin{cases} 0 & \text{if } j \neq j_i^* \\ \frac{1}{n} & \text{if } j = j_i^* \end{cases}.$$

Hence, without fairness constraints, FWC corresponds to Lloyd’s algorithm for clustering. Specifically, Lloyd’s algorithm iteratively computes the centroid for each subset in the partition and subsequently re-partitions the input based on the closeness to these centroids (Lloyd, 1982); these are the same operations FWC does in optimizing the surrogate function and solving problem (16). Thus, when $c(x, y)$ is correspondingly defined as $\|x - y\|_1$ or $\|x - y\|_2^2$, FWC corresponds to Lloyd’s algorithm applied to k-medians or k-means problems, except the centroids have fixed values for \widehat{D} and \widehat{Y} (see Section 3).

5. Experiments

Runtime Analysis Firstly, we evaluate the runtime performance of FWC by creating a synthetic dataset of dimension

n and features of dimension p , with the goal of creating a coreset of size m (see Appendix C.1 for more details). We fix two out of the three parameters to their default values $(n, m, p) = (5000, 250, 25)$ and vary the other across suitable ranges, to analyse the runtime and total number of iterations. Figure 1, top left, shows the runtime and number of iterations when increasing the original dataset sample size n from 1,000 to 50,000 (with average and standard deviation over 10 separate runs); both the runtime and number of iterations grow proportionally to the sample size n , with each iteration running below 2 seconds and a maximum runtime of around 5 minutes. Figure 3 in Appendix C.1 also shows that requiring a larger coreset size m converges faster in terms of number of iterations, but increases the iteration runtime as more representatives need to be computed.

Real Datasets We evaluate the performance of FWC on 4 real datasets widely used in the fairness literature (Fabris et al., 2022): (i) the Adult dataset (Becker & Kohavi, 1996), (ii) the German Credit dataset (Hofmann, 1994), (iii) the Communities and Crime dataset (Redmond, 2009) and (iv) the Drug dataset (Fehrman et al., 2017). For each datasets, we consider 3 different coreset sizes m , 5%, 10% and 20% (apart from the Adult dataset, in which we select m equal to 0.5%, 1% and 2% due to the large dataset size). Across these datasets, we compare with (a) Fairlets and IndFair, two fair clustering approaches by (Backurs et al., 2019) and (Chhaya et al., 2022), (b) K-Median Coresets, a coreset approach by (Bachem et al., 2018), (c) k-means (Lloyd, 1982) and k-medoids (Maranzana, 1963; Park & Jun, 2009), two classic clustering approaches and (d) Uniform Subsampling of the original dataset. For FWC, we consider three different values of the fairness violation hyperparameters ϵ for the optimization problem in (6). Table 1 shows that FWC consistently achieves coresets that are closer in distribution to the original dataset with respect to the other methods. In addition, although FWC is not natively minimizing clustering cost, FWC provides good clustering performance and is competitive in terms of clustering cost for smaller datasets. Note that creating coresets for the Credit datasets is more challenging for FWC due to the high number of discrete features, which makes the minimization non-smooth in the feature space and creates multiple equivalent solutions when solving the dual of problem (10). Finally, we compute the fairness-utility tradeoff by first training a downstream multi-layer perception (MLP) classifier on the coresets created by each approach and then evaluating the classifier demographic disparity (fairness) and AUC (utility). Figure 1 shows the model with the best fairness-utility tradeoff across the three coreset sizes m , for each approach. FWC obtains a smaller disparity at the same accuracy compared to other approaches for the Drug and Adult datasets, and performance remains competitive even when using a fairness pre-processing approach (Kamiran &

	Wasserstein Distance (\downarrow)				Clustering Cost (\downarrow)			
	Adult	Credit	Crime	Drug	Adult	Credit	Crime	Drug
FWC Ranking	1st/1st/1st	1st/3rd/3rd	1st/1st/1st	1st/1st/1st	5 th /5 th /5 th	1st/5th/4th	1st/1st/2nd	1st/1st/2nd

Table 1. Relative ranking of FWC coresets compared to other approaches for Wasserstein distance to the original datasets and clustering cost, across three coreset sizes m . For instance, in the Adult dataset FWC is first (1st) in terms of Wasserstein distance, i.e., the empirical distribution of FWC coresets is closest to the original dataset with respect to any other method, across the three coreset sizes m . Overall, FWC consistently creates coresets that are closer in distribution to the original dataset, and can obtain competitive clustering performance. We use this custom notation for brevity and highlighting the performance with respect to other methods, see Appendix C for more details.

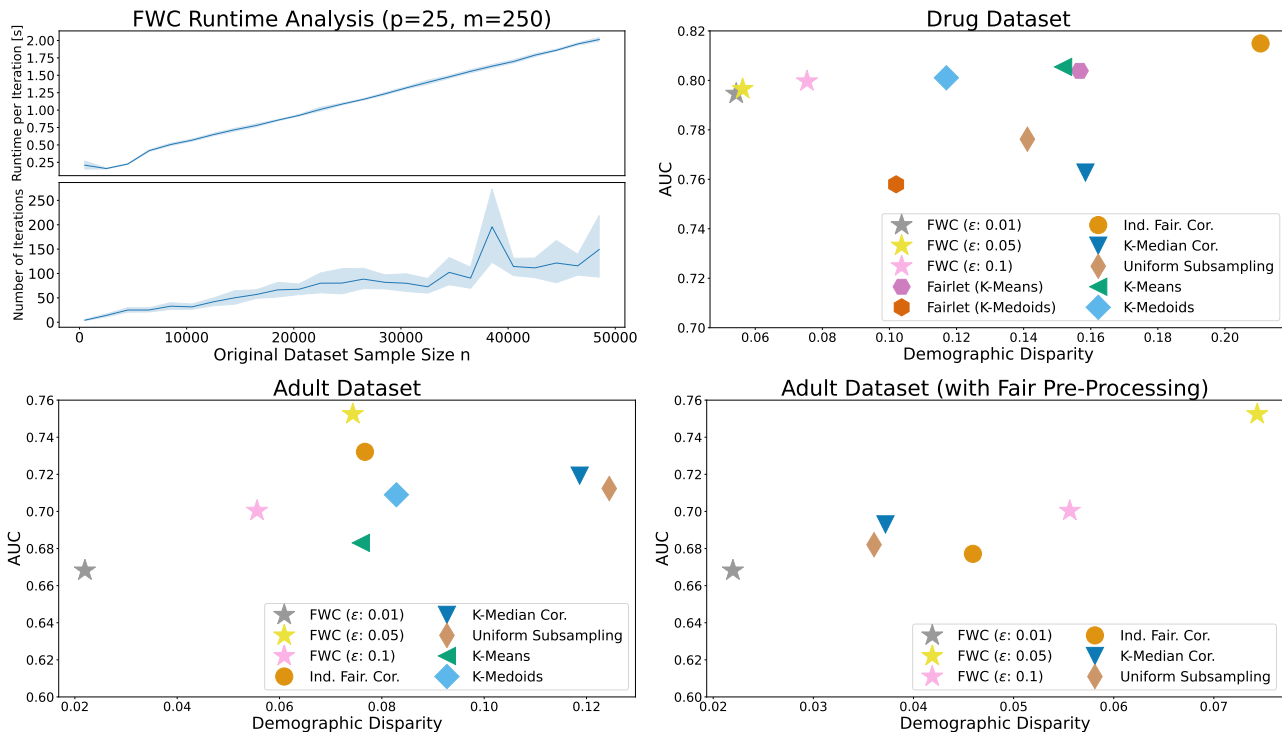


Figure 1. Top left: FWC runtime when changing the original dataset size n . Others: Fairness-utility tradeoff on Drug and Adult datasets for a downstream MLP classifier, selecting the model with the best performance-fairness tradeoff across three different coreset sizes m . FWC consistently achieves a comparable/better tradeoff, even when adjusting the other coresets with a fairness pre-processing technique (Kamiran & Calders, 2012). Averages taken over 10 runs, see Appendix C.2 for standard deviations and more details.

Calders, 2012). See Appendix C.2 for more details.

Data Augmentation Using the same datasets mentioned above, we evaluate the performance of FWC in reducing the downstream demographic disparity when doing data augmentation, i.e., adding the synthetic representatives to the training data when training a downstream model. We use the data augmentation scheme adopted by Sharma et al. (2020, Section 2.1), which first uses k-means on the original dataset and then sorts the synthetic representatives based on the distance of each synthetic representative to the nearest k-mean centroid with the same combination of protected attribute and outcome D and Y . We generate a set of synthetic datasets of size equal to 50% of the original dataset and look at the performance-fairness of a downstream model

trained augmented with such synthetic representative in increments of 5% (20% and 2.5% respectively for the Adult dataset, given the large dataset size). Figure 2 shows the fairness-utility tradeoff of the downstream MLP classifier when doing data augmentation, selecting the best model across various degrees of data augmentation, along with the performance of the baseline MLP classifier with no data augmentation. In all datasets the data augmentation with FWC seem to either increase the performance or reduce the demographic disparity, with the only exception being the Drug dataset. Upon further investigation, the inclusion of the protected attribute D in the downstream model provides a better demographic parity and accuracy than by excluding it, indicating the predictive attribute has a strong predictive power (see Figure 5 in Appendix for more details). We

Adult Dataset	Zero Shot		Few Shot ($b_p = 0$)		Few Shot (FWC)	
	Accuracy	DP	Accuracy	DP	Accuracy	DP
GPT-3.5 Turbo	53.55 \pm 0.87	0.040 \pm 0.017	57.99 \pm 1.88	0.019 \pm 0.015	55.02 \pm 1.26	0.010 \pm 0.03
GPT-4	76.54 \pm 1.63	0.42 \pm 0.016	74.39 \pm 2.86	0.33 \pm 0.09	65.20 \pm 0.85	0.27 \pm 0.04

Table 2. Similar to Wang et al. (2023), we use GPT-3.5 Turbo and GPT-4 LLM’s for fairness evaluations, with a test set of 200 samples with 0.5 base parity ($b_p = 0.5$). Zero shot and few shot represent the same setup as in Wang et al. (2023), where 16 examples are provided to the model with zero base parity in the few shot case. Few Shot - FWC is used to provide sixteen examples with weights to the model as examples. Accuracy and demographic disparity (DP) based on the resulting predictions from GPT-3.5 and GPT-4 models are reported.

Data Augmentation Performance-Fairness Tradeoff, Best Models

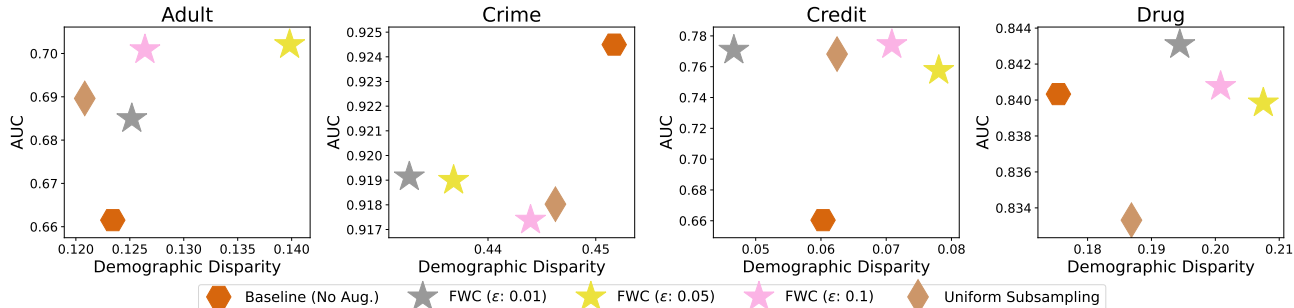


Figure 2. Fairness-utility tradeoff of models trained using coresets as data augmentation, following the strategy from Sharma et al. (2020). Each point shows the best model in terms of tradeoff over various degrees of data augmentation, in addition to the baseline model with no augmentation (averages over 10 runs). FWC seem to either increase the performance or reduce the demographic disparity, with the only exception being the Drug dataset. Further analysis shows that this phenomenon only happens if the protected attribute (gender) is used during training, hence pointing to a strong relationship between protected attributes and outcome; see Appendix C.2 for details.

include more details and a comparison with other coreset approaches in Appendix C.2 and Figures 4 and 6.

Using FWC to improve fairness for GPT-3.5 Turbo and GPT-4 Wang et al. (2023, Section 10.2) evaluate GPT-3.5 and GPT-4 for fairness on predictive tasks for the UCI Adult dataset in a zero and few shot setting. We use a similar evaluation setup as provided and use FWC in the few shot setting as examples and evaluate the results for the gender protected attribute. Specifically, we pass the tabular data as language descriptions to GPT-3.5 Turbo and GPT-4 to perform classification tasks on it. We select 200 samples to construct the test set and use a set of samples found using FWC as examples. Further details on this experiment are provided in the appendix. The results are shown in Table 2. Examples provided by FWC help reduce demographic disparity more than providing balanced few shot examples, while losing on predictive accuracy (note that the drop in accuracy is similar to the drop observed in (Wang et al., 2023) and is representative of the fairness-utility trade-off). Owing to the token limitation of LLM’s, these representative coresets can evidently be valuable to provide a small set of samples that can help mitigate bias. Due to limited availability of computational resources (associated with querying these models), we leave a more thorough evaluation across different datasets and models to future work.

6. Discussion and Conclusions

We introduce FWC, a novel coreset approach that generates synthetic representative samples along with sample-level weights for downstream learning tasks. FWC minimizes the Wasserstein distance between the distribution of the original datasets and that of the weighted synthetic samples, while simultaneously enforcing an empirical version of demographic parity, which ensures the generated samples to be both representative and fair with respect to protected attributes. We demonstrate the effectiveness and scalability of FWC through experiments conducted on both synthetic and real-world datasets. Our results have shown that FWC achieves competitive performance with existing fair clustering and coresets approaches, and can also be used to reduce demographic disparity in LLM predictions (GPT 3.5 and GPT 4). Future extensions include: (i) targeting different fairness metrics such as equalized odds (Hardt et al., 2016; Mishler et al., 2021), (ii) exploring explainability properties of the FWC synthetic representatives (Moshkovitz et al., 2020), (iii) reformulating the optimization framework to target deep neural network pruning (Mussay et al., 2020; Ohib et al., 2022), and (iv) exploring the theoretical fairness guarantees of the FWC coresets by theoretically characterizing the fairness-performance tradeoff (Menon & Williamson, 2018; Li & Liu, 2022; Chzhen & Schreuder, 2022).

Acknowledgements ND is grateful to Alan Mishler for insightful discussions. Some of this work was performed while the first author was at JPMorgan Chase & Co. This paper was prepared for informational purposes by the Artificial Intelligence Research group of JPMorgan Chase & Co. and its affiliates (“J.P. Morgan”), and is not a product of the Research Department of J.P. Morgan. J.P. Morgan makes no representation and warranty whatsoever and disclaims all liability, for the completeness, accuracy or reliability of the information contained herein. This document is not intended as investment research or investment advice, or a recommendation, offer or solicitation for the purchase or sale of any security, financial instrument, financial product or service, or to be used in any way for evaluating the merits of participating in any transaction, and shall not constitute a solicitation under any jurisdiction or to any person, if such solicitation under such jurisdiction or to such person would be unlawful.

References

- Achiam, J., Adler, S., Agarwal, S., Ahmad, L., Akkaya, I., Aleman, F. L., Almeida, D., Altenschmidt, J., Altman, S., Anadkat, S., et al. Gpt-4 technical report. *arXiv preprint arXiv:2303.08774*, 2023.
- Bachem, O., Lucic, M., and Lattanzi, S. One-shot coresets: The case of k-clustering. In *International Conference on Artificial Intelligence and Statistics*, pp. 784–792. PMLR, 2018.
- Backurs, A., Indyk, P., Onak, K., Schieber, B., Vakilian, A., and Wagner, T. Scalable fair clustering. In *International Conference on Machine Learning*, pp. 405–413. PMLR, 2019.
- Becker, B. and Kohavi, R. Adult. UCI Machine Learning Repository, 1996. DOI: <https://doi.org/10.24432/C5XW20>.
- Bertsimas, D. and Tsitsiklis, J. N. *Introduction to linear optimization*, volume 6. Athena scientific Belmont, MA, 1997.
- Black, E., Yeom, S., and Fredrikson, M. Fliptest: fairness testing via optimal transport. In *Proceedings of the 2020 Conference on Fairness, Accountability, and Transparency*, pp. 111–121, 2020.
- Borsos, Z., Mutny, M., and Krause, A. Coresets via bilevel optimization for continual learning and streaming. *Advances in Neural Information Processing Systems*, 33: 14879–14890, 2020.
- Calmon, F., Wei, D., Vinzamuri, B., Natesan Ramamurthy, K., and Varshney, K. R. Optimized pre-processing for discrimination prevention. *Advances in Neural Information Processing Systems*, 30, 2017.
- Campbell, T. and Broderick, T. Bayesian coreset construction via greedy iterative geodesic ascent. In *International Conference on Machine Learning*, pp. 698–706. PMLR, 2018.
- Chhaya, R., Dasgupta, A., Choudhari, J., and Shit, S. On coresets for fair regression and individually fair clustering. In *International Conference on Artificial Intelligence and Statistics*, pp. 9603–9625. PMLR, 2022.
- Chierichetti, F., Kumar, R., Lattanzi, S., and Vassilvitskii, S. Fair clustering through fairlets. *Advances in Neural Information Processing Systems*, 30, 2017.
- Chouldechova, A. Fair prediction with disparate impact: A study of bias in recidivism prediction instruments. *Big Data*, 5(2):153–163, 2017.
- Chzhen, E. and Schreuder, N. A minimax framework for quantifying risk-fairness trade-off in regression. *The Annals of Statistics*, 50(4):2416–2442, 2022.
- Claici, S., Genevay, A., and Solomon, J. Wasserstein measure coresets. *arXiv preprint arXiv:1805.07412*, 2018.
- Coleman, C., Yeh, C., Musmann, S., Mirzasoleiman, B., Bailis, P., Liang, P., Leskovec, J., and Zaharia, M. Selection via proxy: Efficient data selection for deep learning. In *International Conference on Learning Representations*, 2020. URL <https://openreview.net/forum?id=HJg2b0VYDr>.
- Dwork, C., Hardt, M., Pitassi, T., Reingold, O., and Zemel, R. Fairness through awareness. In *Proceedings of the 3rd Innovations in Theoretical Computer Science Conference*, pp. 214–226, 2012.
- Fabris, A., Messina, S., Silvello, G., and Susto, G. A. Algorithmic fairness datasets: The story so far. *Data Mining and Knowledge Discovery*, 36(6):2074–2152, 2022.
- Fehrman, E., Muhammad, A. K., Mirkes, E. M., Egan, V., and Gorban, A. N. The five factor model of personality and evaluation of drug consumption risk. In *Data Science: Innovative Developments in Data Analysis and Clustering*, pp. 231–242. Springer, 2017.
- Feldman, D. Core-sets: Updated survey. *Sampling Techniques for Supervised or Unsupervised Tasks*, pp. 23–44, 2020.
- Ge, Y., Zhao, X., Yu, L., Paul, S., Hu, D., Hsieh, C.-C., and Zhang, Y. Toward pareto efficient fairness-utility trade-off in recommendation through reinforcement learning. In *Proceedings of the fifteenth ACM international conference on web search and data mining*, pp. 316–324, 2022.

- Ghadiri, M., Samadi, S., and Vempala, S. Socially fair k-means clustering. In *Proceedings of the 2021 ACM Conference on Fairness, Accountability, and Transparency*, pp. 438–448, 2021.
- Gordaliza, P., Del Barrio, E., Fabrice, G., and Loubes, J.-M. Obtaining fairness using optimal transport theory. In *International conference on machine learning*, pp. 2357–2365. PMLR, 2019.
- Har-Peled, S. and Mazumdar, S. On coresets for k-means and k-median clustering. In *Proceedings of the thirty-sixth annual ACM symposium on Theory of computing*, pp. 291–300, 2004.
- Hardt, M., Price, E., and Srebro, N. Equality of opportunity in supervised learning. *Advances in neural information processing systems*, 29, 2016.
- Hofmann, H. Statlog (German Credit Data). UCI Machine Learning Repository, 1994. DOI: <https://doi.org/10.24432/C5NC77>.
- Hort, M., Chen, Z., Zhang, J. M., Harman, M., and Sarro, F. Bias mitigation for machine learning classifiers: A comprehensive survey. *ACM J. Responsib. Comput.*, nov 2023. doi: 10.1145/3631326. URL <https://doi.org/10.1145/3631326>.
- Huang, L., Jiang, S., and Vishnoi, N. Coresets for clustering with fairness constraints. *Advances in Neural Information Processing Systems*, 32, 2019.
- Jiang, H., Lee, Y. T., Song, Z., and Wong, S. C.-w. An improved cutting plane method for convex optimization, convex-concave games, and its applications. In *Proceedings of the 52nd Annual ACM SIGACT Symposium on Theory of Computing*, pp. 944–953, 2020.
- Jung, C., Kannan, S., and Lutz, N. A center in your neighborhood: Fairness in facility location. *arXiv preprint arXiv:1908.09041*, 2019.
- Kamiran, F. and Calders, T. Data preprocessing techniques for classification without discrimination. *Knowledge and Information Systems*, 33(1):1–33, 2012.
- Kantorovitch, L. On the translocation of masses. *Management Science*, 5(1):1–4, 1958.
- Khachiyan, L. G. Polynomial algorithms in linear programming. *USSR Computational Mathematics and Mathematical Physics*, 20(1):53–72, 1980.
- Lange, K. *MM optimization algorithms*. SIAM, 2016.
- Lei, S. and Tao, D. A comprehensive survey of dataset distillation. *IEEE Transactions on Pattern Analysis & Machine Intelligence*, 46(01):17–32, jan 2024. ISSN 1939-3539. doi: 10.1109/TPAMI.2023.3322540.
- Li, P. and Liu, H. Achieving fairness at no utility cost via data reweighing with influence. In *International Conference on Machine Learning*, pp. 12917–12930. PMLR, 2022.
- Lloyd, S. Least squares quantization in PCM. *IEEE Transactions on Information Theory*, 28(2):129–137, 1982.
- Mahabadi, S. and Vakilian, A. Individual fairness for k-clustering. In *International Conference on Machine Learning*, pp. 6586–6596. PMLR, 2020.
- Maranzana, F. E. On the location of supply points to minimize transportation costs. *IBM Systems Journal*, 2(2): 129–135, 1963.
- Menon, A. K. and Williamson, R. C. The cost of fairness in binary classification. In Friedler, S. A. and Wilson, C. (eds.), *Proceedings of the 1st Conference on Fairness, Accountability and Transparency*, volume 81 of *Proceedings of Machine Learning Research*, pp. 107–118. PMLR, 23–24 Feb 2018. URL <https://proceedings.mlr.press/v81/menon18a.html>.
- Mishler, A., Kennedy, E. H., and Chouldechova, A. Fairness in risk assessment instruments: Post-processing to achieve counterfactual equalized odds. In *Proceedings of the 2021 ACM Conference on Fairness, Accountability, and Transparency*, pp. 386–400, 2021.
- Moshkovitz, M., Dasgupta, S., Rashtchian, C., and Frost, N. Explainable k-means and k-medians clustering. In III, H. D. and Singh, A. (eds.), *Proceedings of the 37th International Conference on Machine Learning*, volume 119 of *Proceedings of Machine Learning Research*, pp. 7055–7065. PMLR, 13–18 Jul 2020. URL <https://proceedings.mlr.press/v119/moshkovitz20a.html>.
- Mussay, B., Osadchy, M., Braverman, V., Zhou, S., and Feldman, D. Data-independent neural pruning via coresets. In *International Conference on Learning Representations*, 2020. URL <https://openreview.net/forum?id=H1gmHaEKwB>.
- Negahbani, M. and Chakrabarty, D. Better algorithms for individually fair k -clustering. *Advances in Neural Information Processing Systems*, 34:13340–13351, 2021.
- Ohib, R., Gillis, N., Dalmaso, N., Shah, S., Potluru, V. K., and Plis, S. Explicit group sparse projection with applications to deep learning and NMF. *Transactions on Machine Learning Research*, 2022. ISSN 2835-8856. URL <https://openreview.net/forum?id=jIrOeWjdpc>.
- OpenAI. Chatgpt3.5. <https://chat.openai.com>, 2022.

- Ortega, J. M. and Rheinboldt, W. C. *Iterative solution of nonlinear equations in several variables*. SIAM, 2000.
- Park, H.-S. and Jun, C.-H. A simple and fast algorithm for k-medoids clustering. *Expert Systems with Applications*, 36(2):3336–3341, 2009.
- Pedregosa, F., Varoquaux, G., Gramfort, A., Michel, V., Thirion, B., Grisel, O., Blondel, M., Prettenhofer, P., Weiss, R., Dubourg, V., et al. Scikit-learn: Machine learning in python. *Journal of Machine Learning Research*, 12(Oct):2825–2830, 2011.
- Peyré, G., Cuturi, M., et al. Computational optimal transport: With applications to data science. *Foundations and Trends® in Machine Learning*, 11(5-6):355–607, 2019.
- Redmond, M. Communities and Crime. UCI Machine Learning Repository, 2009. DOI: <https://doi.org/10.24432/C53W3X>.
- Sagioglu, S. and Sinanc, D. Big data: A review. In *2013 International Conference on Collaboration Technologies and Systems (CTS)*, pp. 42–47. IEEE, 2013.
- Santambrogio, F. Optimal transport for applied mathematicians. *Birkäuser, NY*, 55(58-63):94, 2015.
- Sharma, S., Zhang, Y., Rios Aliaga, J. M., Bouneffouf, D., Muthusamy, V., and Varshney, K. R. Data augmentation for discrimination prevention and bias disambiguation. In *Proceedings of the AAAI/ACM Conference on AI, Ethics, and Society*, pp. 358–364, 2020.
- Silvia, C., Ray, J., Tom, S., Aldo, P., Heinrich, J., and John, A. A general approach to fairness with optimal transport. In *Proceedings of the AAAI Conference on Artificial Intelligence*, volume 34, pp. 3633–3640, 2020.
- Sloane, M., Moss, E., and Chowdhury, R. A silicon valley love triangle: Hiring algorithms, pseudo-science, and the quest for auditability. *Patterns*, 3(2), 2022.
- Vakilian, A. and Yalciner, M. Improved approximation algorithms for individually fair clustering. In *International Conference on Artificial Intelligence and Statistics*, pp. 8758–8779. PMLR, 2022.
- Villani, C. et al. *Optimal transport: Old and new*, volume 338. Springer, 2009.
- Wang, B., Chen, W., Pei, H., Xie, C., Kang, M., Zhang, C., Xu, C., Xiong, Z., Dutta, R., Schaeffer, R., et al. Decodingtrust: A comprehensive assessment of trustworthiness in gpt models. *Thirty-seventh Conference on Neural Information Processing Systems Datasets and Benchmarks Track*, 2023.
- Xiong, Z., Dalmaso, N., Mishler, A., Potluru, V. K., Balch, T., and Veloso, M. FairWASP: Fast and optimal fair wasserstein pre-processing. *arXiv preprint arXiv:2311.00109*, 2023.
- Yu, R., Liu, S., and Wang, X. Dataset distillation: A comprehensive review. *arXiv preprint arXiv:2301.07014*, 2023.
- Zhang, A., Xing, L., Zou, J., and Wu, J. C. Shifting machine learning for healthcare from development to deployment and from models to data. *Nature Biomedical Engineering*, 6(12):1330–1345, July 2022. ISSN 2157-846X. doi: 10.1038/s41551-022-00898-y. URL <https://www.nature.com/articles/s41551-022-00898-y>.

Appendix

A. Details on updating the surrogate function (line 4)

To update the surrogate function, we need to solve problem (10), which is a huge-scale linear program with $O(n)$ constraints and $O(mn)$ nonnegative variables. In this work, we adapt `FairWASP` (Xiong et al., 2023) for cases where $m \neq n$, as opposed to the scenario where $m = n$, which was tackled by Xiong et al. (2023). Before showing the main idea of the algorithm, we rephrase a useful lemma for doing linear minimization on $S_{n,m} \stackrel{\text{def.}}{=} \{P \in \mathbb{R}^{n \times m} : P\mathbf{1}_m = \frac{1}{n} \cdot \mathbf{1}_n, P \geq 0\}$.

Lemma A.1. *For the function $G(C) \stackrel{\text{def.}}{=} \max_{P \in S_{n,m}} \langle C, P \rangle$, it is a convex function of C in $\mathbb{R}^{n \times m}$. For each $i \in [n]$, let $C_{ij_i^*}$ denote a largest component on the i -th row of C , then $G(C) = \frac{1}{n} \sum_{i=1}^n C_{ij_i^*}$. Define the components of P^* as follows:*

$$P_{ij}^* = \begin{cases} 0 & \text{if } j \neq j_i^* \\ \frac{1}{n} & \text{if } j = j_i^* \end{cases} \quad (17)$$

and then $P^* \in \arg \max_{P \in S_{n,m}} \langle C, P \rangle$ and $P^* \in \partial G(C)$.

Proof. The proof of the above lemma is equivalent with that of Lemma 1 of Xiong et al. (2023) in the case when $m \neq n$, which can be extended directly. \square

With this lemma, now we show how to efficiently solve problem (10) via its dual problem. Although (10) is of large scale and computationally prohibitive, it is equivalent to the following saddle point problem on the Lagrangian:

$$\min_{P \in S_{n,m}} \max_{\lambda \in \mathbb{R}_+^h} L(P, \lambda) \stackrel{\text{def.}}{=} \langle C, P \rangle - \lambda^\top A P^\top \mathbf{1}_n \quad (18)$$

where h is the number of rows of A , which is at most $2|\mathcal{Y}||\mathcal{D}|$. It should be mentioned that h is significantly smaller than mn ; for example, for classification tasks with only two protected variables, h is no larger than 8, independent with the number of samples or features. Since $L(\cdot, \cdot)$ is bilinear, the minimax theorem guarantees that (18) is equivalent to $\max_{\lambda \in \mathbb{R}_+^h} \min_{P \in S_{n,m}} L(P, \lambda)$. This is further equal to the dual problem:

$$\max_{\lambda \in \mathbb{R}_+^h} - \left[G(\lambda) \stackrel{\text{def.}}{=} \max_{P \in S_{n,m}} \left\langle \sum_{j=1}^h \lambda_j \mathbf{1}_n a_j^\top - C, P \right\rangle \right], \quad (19)$$

in which a_j^\top denotes the j -th row of A . Note that the problem (19) has much fewer decision variables than that of (18) and Lemma A.1 ensures the function $G(\cdot)$ is convex and has easily accessible function values and subgradients. Therefore, directly applying a cutting plane method has low per-iteration complexity and solves the problem (19) in linear time. We include the details on the cutting plane method in Section A.1 below. Finally, the primal optimal solution of (10) can be easily recovered from the dual optimal solution λ^* via solving $\max_{P \in S_{n,m}} \langle \sum_{j=1}^h \lambda_j^* \mathbf{1}_n a_j^\top - C, P \rangle$, under the assumption that this problem has a unique minimizer, which almost always holds in practice for the computed λ^* and is also assumed by Xiong et al. (2023). In this way, we have shown how the problem (10) can be efficiently solved by applying a cutting plane method on its dual problem.

A.1. Details of the Cutting Plane Method for Solving (19)

The cutting plane method is designed for convex problems where a *separation oracle* can be employed (Khachiyan, 1980). For any $\lambda \in \mathbb{R}^m$, a separation oracle operates by generating a vector g which satisfies $g^\top \lambda \geq g^\top \lambda^*$ for all λ^* in the set of optimal solutions. By repeatedly applying the separation oracle to cut down the potential possible feasible set, the cutting plane method progressively narrows down the feasible solution space until it reaches convergence. The specific steps of the cutting plane algorithm are detailed in Algorithm 2, with the key distinctions among different versions of this method lying in how lines 3 and 4 are implemented.

For the problem (19), a separation oracle (line 4 in Algorithm 2) can directly use the vector of subgradients, which are efficiently accessible, as we mentioned in section 4. Given that we have shown (19) is a low-dimensional convex program with subgradient oracles, there exist many well-established algorithms that can be used. Suppose that the norm of an optimal

Algorithm 2 General Cutting Plane Method for (19)

- 1: Choose a bounded set E_0 that contains an optimal solution
 - 2: **for** k from 0 to n **do**
 - 3: Choose an interior point λ^k of E_k ;
 - 4: Compute $g \in \mathbb{R}^m$ such that

$$g^\top \lambda^k \geq g^\top \lambda^* \text{ for any optimal solution } \lambda^*;$$
 - 5: Choose the next bounded set $E_{k+1} \supseteq \{\lambda \in E_k : g^\top \lambda \leq g^\top \lambda^k\}$;
 - 6: **end for**
-

λ^* is bounded by R , to the best of our knowledge, the cutting plane method with the best theoretical complexity is given by Jiang et al. (2020), who proposed an improved cutting plane method that only needs $O((h \cdot \text{SO} + h^2) \cdot \log(hR/\epsilon))$ flops. Here SO denotes the complexity of the separation oracle. Note that here h is at most $2|\mathcal{D}||\mathcal{Y}|$ and far smaller than n or m . Here we restate the Corollary 5 of Xiong et al. (2023) below for the overall time and space complexity of applying the cutting plane method in the case $m = n$.

Lemma A.2 (Corollary 5 of Xiong et al. (2023)). *With efficient computation and space management, when $m = n$, the cutting plane method solves the problem (19) within*

$$\tilde{O}(n^2 + |\mathcal{D}|^2 |\mathcal{Y}|^2 n \cdot \log(R/\epsilon)) \quad (20)$$

flops and $O(n|\mathcal{D}||\mathcal{Y}|)$ space. Here we use $\tilde{O}(\cdot)$ to hide m , n , $|\mathcal{D}|$, and $|\mathcal{Y}|$ in the logarithm function.

It should be noted that in the general case $m \neq n$, the above results can also be generalized via a similar proof. For our case $m \ll n$, the complexity can be further decreased and the term n^2 in (20) can be replaced with mn . Finally, in terms of the implementation, we follow Xiong et al. (2023) and use the analytic center cutting plane method.

B. Theoretical Proofs

This section includes the theoretical proofs for Section 3 and Section 4.3, where we show (i) the optimization problem can be reduced to optimizing over the \hat{X} rather than \hat{Z} (Lemma 3.1), (ii) the surrogate function is convex and a valid upper bound of the optimization objective (Lemma 4.1), (iii) our proposed algorithm converges to a first-order stationary point in \hat{X} (Theorem 4.2), and (iv) our proposed algorithm terminates in a finite amount of iterations (Theorem 4.3).

Proof of Lemma 3.1. Once we generate $m|\mathcal{D}||\mathcal{Y}|$ data points, the feasible set of the latter Wasserstein coreset contains the feasible set of the former Wasserstein coreset. \square

Proof of Lemma 4.1. The convexity follows directly from the convexity of $C(\hat{X})$, as the $P_k^* \geq 0$ in (12).

Before proving it is an upper bound, we show some important properties of $F(C)$ as a function of C . Firstly, $F(C)$ is concave on C because of the concavity of the minimum LP's optimal objective on the objective vector. Secondly, since the feasible set of problem (10) is bounded, the optimal solution $F(C)$ is continuous with respect to C . Thirdly, due to the sensitivity analysis of LP (Bertsimas & Tsitsiklis, 1997), a supergradient of $F(C)$ at point C is the corresponding optimal solution P^* . Here the definition of supergradients for concave functions is analogous to the definition of subgradients for convex functions.

Now we prove $g(\hat{X}; \hat{X}^k)$ is an upper bound of $F(C(\hat{X}))$. Because P_k^k is a supergradient of $F(C)$ when $C = C(\hat{X}^k)$,

$$F(C) + \langle P_k^k, C(\hat{X}) - C \rangle \geq F(C(\hat{X}^k)),$$

in which the left-hand side is equal to $g(\hat{X}; \hat{X}^k)$ because $F(C) = \langle P_k^k, C \rangle$ and $g(\hat{X}; \hat{X}^k) = \langle C(\hat{X}), P_k^* \rangle$. Therefore, the surrogate function is an upper bound of the objective function $F(C(\hat{X}))$, i.e., $g(\hat{X}; \hat{X}^k) \geq F(C(\hat{X}))$. Moreover, due to the definition in (12), $g(\hat{X}; \hat{X}^k) = F(C(\hat{X}))$ when $\hat{X} = \hat{X}^k$. \square

Proof of Theorem 4.2. The monotonically decreasing part of the claim follows by:

$$F(C(\hat{X}^{k+1})) \leq g(\hat{X}^{k+1}; \hat{X}^k) = \arg \min_{\hat{X} \in \mathcal{X}^m} g(\hat{X}; \hat{X}^k) \leq g(\hat{X}^k; \hat{X}^k) = F(C(\hat{X}^k)). \quad (21)$$

Here the first inequality is due to the fact that $g(\widehat{X}; \widehat{X}^k) \geq F(C(\widehat{X}))$ for any \widehat{X} . The final equality is because $g(\widehat{X}; \widehat{X}^k) = F(C(\widehat{X}))$ when $\widehat{X} = \widehat{X}^k$. Once $g(\widehat{X}^k; \widehat{X}^k) = g(\widehat{X}^{k+1}; \widehat{X}^k)$ and thus $\widehat{X}^k \in \arg \min_{\widehat{X} \in \mathcal{X}^m} g(\widehat{X}; \widehat{X}^k)$, then \widehat{X}^k is a global minimizer of the convex upper bound $g(\cdot; \widehat{X}^k)$ for $F(C(\cdot))$ and the upper bound $g(\widehat{X}^k; \widehat{X}^k)$ attains the same function value with $F(C(\widehat{X}^k))$. Therefore, if the surrogate function is smooth at \widehat{X}^k , which could be achieved if $C(\widehat{X}^k)$ is smooth at \widehat{X}^k , then X^k is a first-order stationary point of (11). \square

Proof of Theorem 4.3. Because (13) has a unique minimizer, the second inequality in (21) holds strictly when $\widehat{X}^{k+1} \neq \widehat{X}^k$, or equivalently $g(\widehat{X}^{k+1}; \widehat{X}^k) \neq g(\widehat{X}^k; \widehat{X}^k)$. Once $\widehat{X}^{k+1} = \widehat{X}^k$, then the algorithm terminates. Note that there are only finite possible optimal basic feasible solution P^* that could be generated by FairWASP, as shown in Lemma A.1. However, before the majority minimization converges, (21) holds strictly and the corresponding P_k^* keeps changing. Therefore, after finite iterations, there must be a P_t^* equal to a previous P_j^* for $j < t$. When that happens, because the surrogate functions are the same and thus have the same minimizer, $\widehat{X}^{t+1} = \widehat{X}^{j+1}$, and the inequalities (21) then hold at equality when $k = j, j + 1, \dots, t$. This implies that $g(\widehat{X}^{j+1}; \widehat{X}^j) = g(\widehat{X}^j; \widehat{X}^j)$, so the algorithm terminates within finite iterations. \square

C. Experiment Details

C.1. Runtime Analysis on Synthetic Dataset

As mentioned in Section 5, we generate a synthetic dataset in which one feature is strongly correlated with the protected attribute D to induce a backdoor dependency on the outcome. We consider a binary protected attribute, $D \in \{0, 1\}$, which could indicate e.g., gender or race. The synthetic dataset contains two features, a feature X_1 correlated with the protected attribute and a feature X_2 uncorrelated with the protected attribute. For $D = 0$, X_1 is uniformly distributed in $[0, 10]$, while for $D = 1$, $X_1 = 0$. Instead, X_2 is 5 times a random variable from a normal distribution $\mathcal{N}(0, 1)$. Finally, the outcome Y is binary, so $Y = \{0, 1\}$: $Y_i = 1$ when $Y_i > m_x + \epsilon_i$ and $Y_i = 0$ when $Y_i \leq m_x + \epsilon_i$, where m_x is the mean of $\{(X_1)_i + (X_2)_i\}_i$ and the noise ϵ_i comes from a normal distribution $\mathcal{N}(0, 1)$.

This experiment visualizes the speed of our method with respect to different numbers of overall samples n , number of samples in the compressed dataset m , and the dimensionality of features p . We evaluated the performance of the algorithm under the synthetic data with different configurations of n , p , and m . In this experiment, we set compute the fair Wasserstein coreset under the l_1 -norm distance and we use k-means (Lloyd, 1982) to initialize the starting coreset \widehat{X}^0 . We terminate the algorithm when $\widehat{X}^k = \widehat{X}^{k-1}$. The time per iteration and total iterations for varying n , p , and m are shown in the Figures 1 (top left) and 3. We see that increasing the sample size of the original dataset n increases the runtime and number of iterations (keeping them within a maximum of 5 minutes), while increasing the number of coresets m or dimensionality of the features p reduces the overall numbers of iterations but increases each iteration’s runtime.

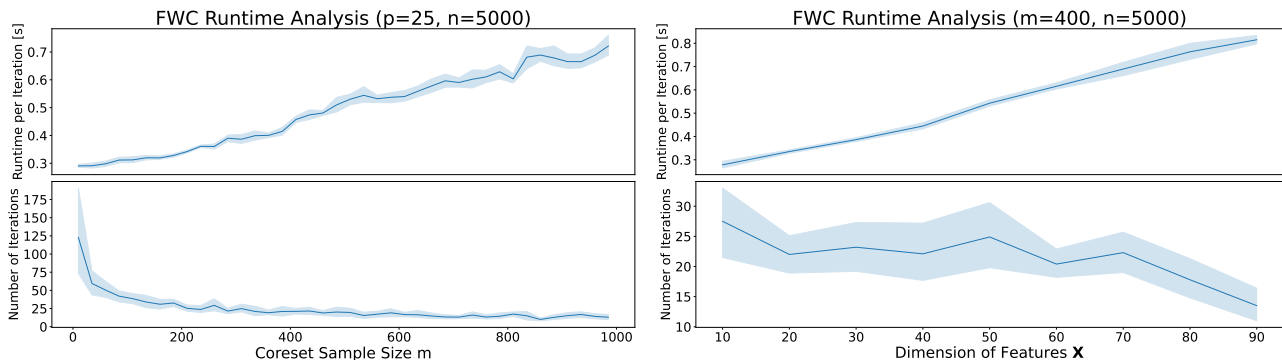


Figure 3. Runtime analysis of FWC when varying the size of the coreset m (left) and the dimensionality of the features p (right). We report averages and one standard deviation computed over 10 runs.

C.2. Real Datasets

We consider the following four real datasets widely used in the fairness literature (Fabris et al., 2022):

- the *Adult dataset* (Becker & Kohavi, 1996), which reports demographic data from the 1994 US demographic survey

Fair Coresets via Optimal Transport

Method	Wasserstein Distance (\downarrow)				Clustering Cost (\downarrow)			
	Adult	Credit	Crime	Drug	Adult	Credit	Crime	Drug
FWC (ϵ : 0.01)	2 nd /1 st /1 st	1 st /5 th /6 th	1 st /2 nd /3 rd	1 st /2 nd /6 th	6 th /5 th /5 th	1 st /7 th /9 th	1 st /4 th /7 th	1 st /6 th /7 th
FWC (ϵ : 0.05)	1 st /2 nd /2 nd	6 th /3 rd /4 th	3 rd /1 st /2 nd	4 th /1 st /2 nd	5 th /6 th /7 th	8 th /5 th /6 th	4 th /1 st /4 th	4 th /1 st /6 th
FWC (ϵ : 0.1)	3 rd /3 rd /3 rd	4 th /6 th /3 rd	2 nd /3 rd /1 st	2 nd /4 th /1 st	7 th /7 th /6 th	6 th /8 th /4 th	2 nd /7 th /2 nd	2 nd /8 th /2 nd
Fairlet (K-Means)	-/-	9 th /9 th /7 th	5 th /7 th /4 th	5 th /6 th /4 th	-/-	3 rd /2 nd /2 nd	5 th /3 rd /3 rd	5 th /5 th /3 rd
Fairlet (K-Medoids)	-/-	8 th /8 th /9 th	10 th /10 th /10 th	10 th /10 th /10 th	-/-	10 th /10 th /10 th	10 th /10 th /10 th	10 th /10 th /9 th
Ind. Fair. Cor.	4 th /6 th /5 th	2 nd /4 th /1 st	6 th /8 th /5 th	6 th /9 th /7 th	2 nd /4 th /2 nd	4 th /6 th /3 rd	6 th /9 th /6 th	6 th /9 th /5 th
K-Median Cor.	6 th /4 th /6 th	3 rd /1 st /2 nd	7 th /6 th /8 th	8 th /7 th /9 th	4 th /2 nd /3 rd	5 th /3 rd /5 th	9 th /6 th /9 th	9 th /4 th /10 th
Uniform Subsampling	5 th /5 th /4 th	5 th /2 nd /5 th	8 th /5 th /7 th	9 th /5 th /8 th	3 rd /3 rd /4 th	7 th /4 th /7 th	8 th /5 th /8 th	8 th /2 nd /8 th
K-Means	7 th /8 th /8 th	10 th /10 th /10 th	4 th /4 th /6 th	3 rd /3 rd /3 rd	1 st /1 st /1 st	2 nd /1 st /1 st	3 rd /2 nd /1 st	3 rd /3 rd /1 st
K-Medoids	8 th /7 th /7 th	7 th /7 th /8 th	9 th /9 th /9 th	7 th /8 th /5 th	8 th /8 th /8 th	9 th /9 th /8 th	7 th /8 th /5 th	7 th /7 th /4 th

Table 3. Ranking of coresets created by each methods in terms of Wasserstein distance to the original datasets and clustering cost, for each of the three coreset sizes m . FWC consistently creates coresets that are closer in distribution to the original dataset and performs competitively in terms of clustering costs for small datasets, although not natively minimizing clustering costs. For numeric values, see Tables 4 and 5.

about $\sim 49,000$ individuals. We use all the available features for classification apart from the “fnlwtg” feature, including gender as the protected attribute D and whether the individual salary is more than USD50,000;

- the *Drug dataset* (Fehrman et al., 2017), which contains drug usage history for 1,885 individuals. Features X include the individual age, country of origin, education and scores on various psychological test. We use the individual gender as the protected variable D . The response Y is based on whether the individual has reported to have ever used the drug “cannabis” or not;
- the *Communities and Crime dataset* (Redmond, 2009) was put together towards the creation of a software tool for the US police department. The dataset contains socio-economic factors for $\sim 2,000$ communities in the US, along with the proportion of violent crimes in each community. As protected attribute D , we include whether the percentage of the black population in the community is above the overall median. For the response Y , we use a binary indicator of whether the violent crimes percentage level is above the mean across all communities in the dataset;
- the *German Credit dataset* (Hofmann, 1994) reports a set of 1,000 algorithmic credit decisions from a regional bank in Germany. We use all the available features, including gender as protected attribute D and whether the credit was approved as response Y .

We also include the implementation and hyper-parameters of the methods used in the fairness-utility tradeoffs presented in Figures 1, 2, 4, 5, 6, 7 and 8:

- For FWC we set the fairness violation hyper-parameter ϵ of problem in Equation (6) to be $\epsilon = [0.01, 0.05, 0.1]$, hence obtaining three separate FWC models, FWC (0.01), FWC (0.05) and FWC (0.1);
- For Fairlet (Backurs et al., 2019), we use the implementation available at the following GitHub repository: https://github.com/talwagner/fair_clustering/tree/master
- For IndFair (Chhaya et al., 2022) and K-Median Coresets (Bachem et al., 2018), we use the implementation available at the following GitHub repository: <https://github.com/jayeshchoudhari/CoresetIndividualFairness/tree/master>
- For k-means (Lloyd, 1982) and k-medoids (Maranzana, 1963; Park & Jun, 2009) we use the implementations available in the Python package Scikit-Learn (Pedregosa et al., 2011)

All computations are run on an Ubuntu machine with 32GB of RAM and 2.50GHz Intel(R) Xeon(R) Platinum 8259CL CPU. For all datasets, we randomly split 75% of the data into training/test set, and change the split during each separate

Fair Coresets via Optimal Transport

Method	Wasserstein Distance (\downarrow)											
	Adult ($\times 10^6$)			Credit ($\times 10^6$)			Crime			Drug		
	0.5%	1%	2%	5%	10%	20%	5%	10%	20%	5%	10%	20%
FWC (ϵ : 0.01)	5.72 \pm 0.95	3.76 \pm 0.80	2.70 \pm 0.56	0.40 \pm 0.10	0.75 \pm 0.21	1.07 \pm 0.28	1.65 \pm 0.08	1.76 \pm 0.09	1.89 \pm 0.08	3.23 \pm 0.23	3.57 \pm 0.24	3.98 \pm 0.22
FWC (ϵ : 0.05)	5.57 \pm 0.73	3.90 \pm 0.82	2.79 \pm 0.58	1.07 \pm 0.28	0.48 \pm 0.24	0.72 \pm 0.17	1.87 \pm 0.11	1.66 \pm 0.12	1.72 \pm 0.06	3.95 \pm 0.30	3.31 \pm 0.34	3.49 \pm 0.19
FWC (ϵ : 0.1)	6.18 \pm 1.07	4.15 \pm 0.82	3.04 \pm 0.63	0.71 \pm 0.15	1.05 \pm 0.30	0.47 \pm 0.19	1.70 \pm 0.07	1.85 \pm 0.11	1.62 \pm 0.08	3.50 \pm 0.21	3.95 \pm 0.29	3.25 \pm 0.24
Fairlet (K-Means)	-	-	-	10.02 \pm 2.14	7.47 \pm 2.77	5.00 \pm 2.48	2.10 \pm 0.42	2.10 \pm 0.44	2.00 \pm 0.36	4.29 \pm 0.44	4.10 \pm 0.45	3.83 \pm 0.43
Fairlet (K-Medoids)	-	-	-	3.16 \pm 0.81	4.48 \pm 0.89	5.47 \pm 0.65	4.21 \pm 0.17	4.14 \pm 0.14	4.10 \pm 0.06	6.50 \pm 0.45	5.90 \pm 0.47	5.17 \pm 0.43
Ind. Fair. Cor.	12.96 \pm 5.83	23.91 \pm 25.39	11.48 \pm 8.19	0.41 \pm 0.29	0.72 \pm 0.46	0.23 \pm 0.12	2.35 \pm 0.16	2.60 \pm 0.25	2.01 \pm 0.09	4.84 \pm 0.33	5.51 \pm 0.50	4.17 \pm 0.21
K-Median Cor.	22.11 \pm 17.42	9.37 \pm 11.27	12.04 \pm 9.11	0.66 \pm 0.74	0.26 \pm 0.17	0.36 \pm 0.17	2.58 \pm 0.20	2.01 \pm 0.11	2.35 \pm 0.12	5.38 \pm 0.54	4.16 \pm 0.22	4.80 \pm 0.15
Uniform Subsampling	18.01 \pm 18.34	14.39 \pm 14.90	7.96 \pm 5.42	0.74 \pm 0.53	0.30 \pm 0.16	0.80 \pm 1.15	2.60 \pm 0.26	1.95 \pm 0.13	2.28 \pm 0.24	5.46 \pm 0.59	4.01 \pm 0.30	4.75 \pm 0.42
K-Means	43.96 \pm 18.82	77.04 \pm 18.06	74.50 \pm 12.53	13.23 \pm 1.42	10.76 \pm 1.55	7.59 \pm 1.58	2.00 \pm 0.12	1.93 \pm 0.11	2.04 \pm 0.08	3.94 \pm 0.17	3.66 \pm 0.20	3.62 \pm 0.32
K-Medoids	50.87 \pm 4.30	53.31 \pm 1.85	51.77 \pm 1.86	2.59 \pm 0.42	4.25 \pm 0.68	5.18 \pm 0.07	3.15 \pm 0.08	3.12 \pm 0.11	2.83 \pm 0.06	5.14 \pm 0.08	4.53 \pm 0.28	3.91 \pm 0.09

Table 4. Wasserstein distance of the weighted coresets with respect to the original dataset, with averages and standard deviations obtained over 10 runs. In bold, coresets with the closest distance to the original dataset (i.e., smallest Wasserstein distance) in each coreset size and dataset combination.

Method	Clustering Cost (\downarrow)											
	Adult ($\times 10^6$)			Credit ($\times 10^4$)			Crime ($\times 10^2$)			Drug ($\times 10^2$)		
	0.5%	1%	2%	5%	10%	20%	5%	10%	20%	5%	10%	20%
FWC (ϵ : 0.01)	14.73 \pm 6.43	5.44 \pm 2.29	2.07 \pm 0.39	1.07 \pm 0.21	2.61 \pm 0.59	4.31 \pm 0.92	3.86 \pm 0.27	4.44 \pm 0.21	4.79 \pm 0.19	5.54 \pm 0.41	6.45 \pm 0.32	7.02 \pm 0.31
FWC (ϵ : 0.05)	13.59 \pm 4.21	5.81 \pm 2.37	2.26 \pm 0.30	4.41 \pm 1.52	1.39 \pm 0.96	2.44 \pm 0.21	4.72 \pm 0.36	3.96 \pm 0.41	4.37 \pm 0.14	6.94 \pm 0.54	5.70 \pm 0.63	6.35 \pm 0.24
FWC (ϵ : 0.1)	20.29 \pm 12.27	6.31 \pm 2.36	2.19 \pm 0.29	2.48 \pm 0.20	4.00 \pm 1.28	1.22 \pm 0.41	4.36 \pm 0.15	4.72 \pm 0.34	3.89 \pm 0.30	6.36 \pm 0.26	6.94 \pm 0.51	5.62 \pm 0.45
Fairlet (K-Means)	-	-	-	1.36 \pm 0.09	0.76 \pm 0.11	0.60 \pm 0.31	4.76 \pm 0.46	4.36 \pm 0.52	3.92 \pm 0.56	7.08 \pm 0.30	6.45 \pm 0.40	5.76 \pm 0.63
Fairlet (K-Medoids)	-	-	-	5.79 \pm 1.36	5.40 \pm 1.08	5.04 \pm 0.92	6.27 \pm 0.28	6.00 \pm 0.27	5.59 \pm 0.20	8.58 \pm 0.41	7.93 \pm 0.42	7.09 \pm 0.54
Ind. Fair. Cor.	1.23 \pm 0.37	4.67 \pm 9.46	0.70 \pm 0.04	1.50 \pm 0.38	2.46 \pm 0.77	0.74 \pm 0.10	5.24 \pm 0.27	5.64 \pm 0.48	4.53 \pm 0.22	7.29 \pm 0.35	7.92 \pm 0.62	6.30 \pm 0.41
K-Median Cor.	10.45 \pm 14.21	0.70 \pm 0.04	1.06 \pm 0.19	2.47 \pm 0.90	0.76 \pm 0.06	1.37 \pm 0.29	5.64 \pm 0.39	4.55 \pm 0.27	5.21 \pm 0.16	7.75 \pm 0.66	6.26 \pm 0.36	7.26 \pm 0.20
Uniform Subsampling	10.16 \pm 15.13	3.49 \pm 1.18	1.93 \pm 0.67	3.38 \pm 1.42	1.09 \pm 0.26	2.74 \pm 2.71	5.61 \pm 0.45	4.46 \pm 0.34	5.07 \pm 0.37	7.74 \pm 0.73	6.06 \pm 0.51	7.02 \pm 0.50
K-Means	0.72 \pm 0.01	0.58 \pm 0.01	0.48 \pm 0.01	1.28 \pm 0.21	0.68 \pm 0.12	0.51 \pm 0.29	4.52 \pm 0.16	4.09 \pm 0.25	3.76 \pm 0.39	6.86 \pm 0.28	6.13 \pm 0.41	5.61 \pm 0.67
K-Medoids	83.53 \pm 13.86	75.10 \pm 7.22	56.95 \pm 9.17	4.93 \pm 0.53	4.70 \pm 0.48	4.19 \pm 0.13	5.52 \pm 0.07	5.15 \pm 0.28	4.49 \pm 0.25	7.65 \pm 0.12	6.83 \pm 0.43	5.93 \pm 0.30

Table 5. Clustering cost of the coresets with respect to the original dataset, with averages and standard deviations obtained over 10 runs. In bold, coresets with the smallest clustering cost (i.e., smallest sum of square distances of original dataset samples from the closest generated coreset sample) in each coreset size and dataset combination.

run; the training data are further separated into training and validation with 90/10 to compute early stopping criteria during training. The downstream classifier used is a one-layer deep multi-layer perceptron (MLP) with 20 hidden layers, ReLU activation function in the hidden layer and softmax activation function in the final layer. Unless stated otherwise, FWC uses the L^1 to compute the distance from the original datasets in the optimization problem. For the downstream classifier, the learning rate is set to 10^{-3} , with a batch size of 32, a maximum number of epochs set to 500 with early stopping evaluated on the separate validation set with a patience of 10 epochs and both the features X and the protected attribute D are used for training the classifier. Note that due to the size of the Adult dataset, Fairlet coresets (Backurs et al., 2019) could not be run due to the RAM memory required exceeding the machine capacity (32GB).

Closeness to the original dataset and clustering performance Tables 3, 4 and 5 include the ranking and numerical values (means and standard deviations computed over 10 runs) for all methods in terms of Wasserstein distance from the original dataset and clustering cost, for the three coreset sizes $m = [5\%, 10\%, 20\%]$ (apart from the Adult dataset, in which coreset sizes are set to $m = [0.5\%, 1\%, 2\%]$ due to the large size of the original dataset). Clustering cost is computed as the sum of the squared distance of each points in the original dataset from the closest coreset representative, while the Wasserstein distance is computed solving the optimal transport between the empirical distribution of the original dataset and the one of the coresets, using the L^1 norm as cost function. FWC consistently provides the closest distributional distance to the original dataset in Wasserstein distance, with the only exception of the Credit dataset, in which the large number of discrete features makes the optimization non-smooth in feature space, resulting in a potentially imprecise solution of Equation (11). In addition, FWC, while not naturally minimizing clustering costs, seems to achieve competitive clustering costs in smaller datasets while not performing as well on larger datasets such as Adult.

Fairness-utility tradeoff when using coresets for data augmentation Figure 4 shows the fairness-utility tradeoff for the data augmentation setting in Figure 2, but including standard deviations (obtained over 10 separate runs). Demographic disparity is computed as the following absolute difference:

$$|p(h(X, D) = 1|D = 1) - p(h(X, D) = 1|D = 0)|,$$

for a given classifier h and a protected attribute D with two levels. FWC coresets successfully decrease the demographic disparity or increase the performance (measured with AUC) in the Adult, Crime and Credit datasets, while failing to do so in the Drug dataset. Figure 5 show this effect does not appear if the protected attribute D (gender) is not included in the features used to trained the downstream MLP classifier. This phenomenon indicates the protected attribute provides a strong predictive effect on the outcome (whether the individual has tried cannabis or not), which might potentially be mediated by unmeasured confounders, i.e., other features regarding the recorded individuals which are not available in the Drug dataset. This would require either in-training or post-processing fairness approaches to be alleviated; see Hort et al. (2023) for a comprehensive review on different potential approaches.

As in Figure 8, the standard deviations for Adult and Credit dataset are large due to the downstream model becoming trivial. In addition, Figure 6 provides the same visualizations as Figure 2 (top panel) and Figure 4 (bottom panel), but including all methods mentioned in Section 5. FWC coresets achieve competitive results across the board on all datasets, being part of the so called ‘‘Pareto frontier’’ of the fairness-utility tradeoff (Ge et al., 2022), i.e., either having the best utility or best fairness (or both) among all the approaches considered.

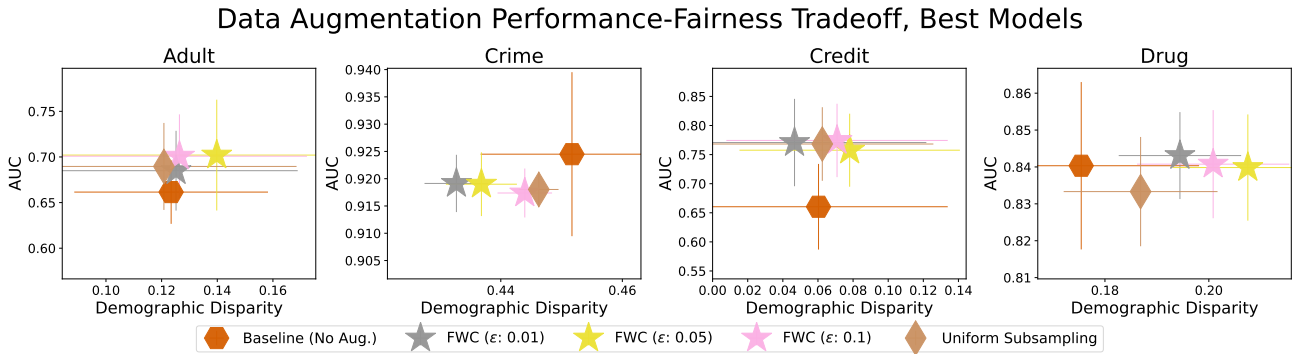


Figure 4. Fairness-utility tradeoff of downstream MLP classifier trained using the original training set augmented with coresets representatives, following the augmentation strategy from Sharma et al. (2020). Each point shows the best model in terms of fairness-utility tradeoff over various degrees of data augmentation, in addition to the baseline model with no augmentation. Means and standard deviations taken over 10 runs.

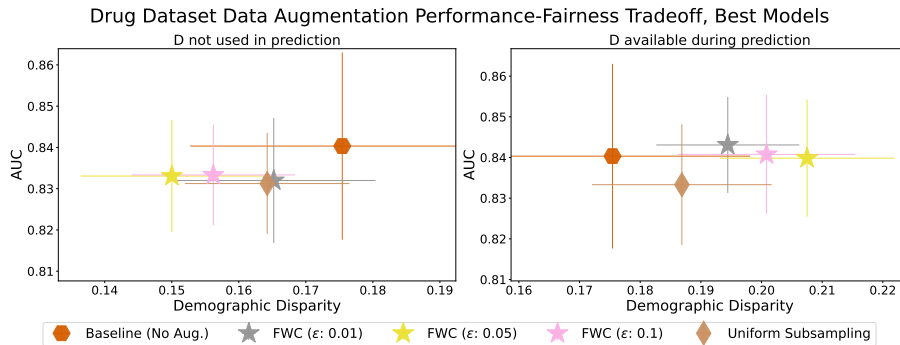


Figure 5. Fairness-utility tradeoff of downstream MLP classifier for the Drug dataset when the protected attribute D (gender) is either not included (left) or included (right) as feature in the learning process. As in Figure 4, the best model across various data augmentation degrees is reported, with averages and standard deviations obtained over 10 runs. FWC coresets manage to successfully reduce the demographic disparity when gender is not used as feature, but fail to do so when gender is used, indicating gender provides strong predictive power for the outcome in question, which would require enforcing fairness either during model training or by post-processing the outputs.

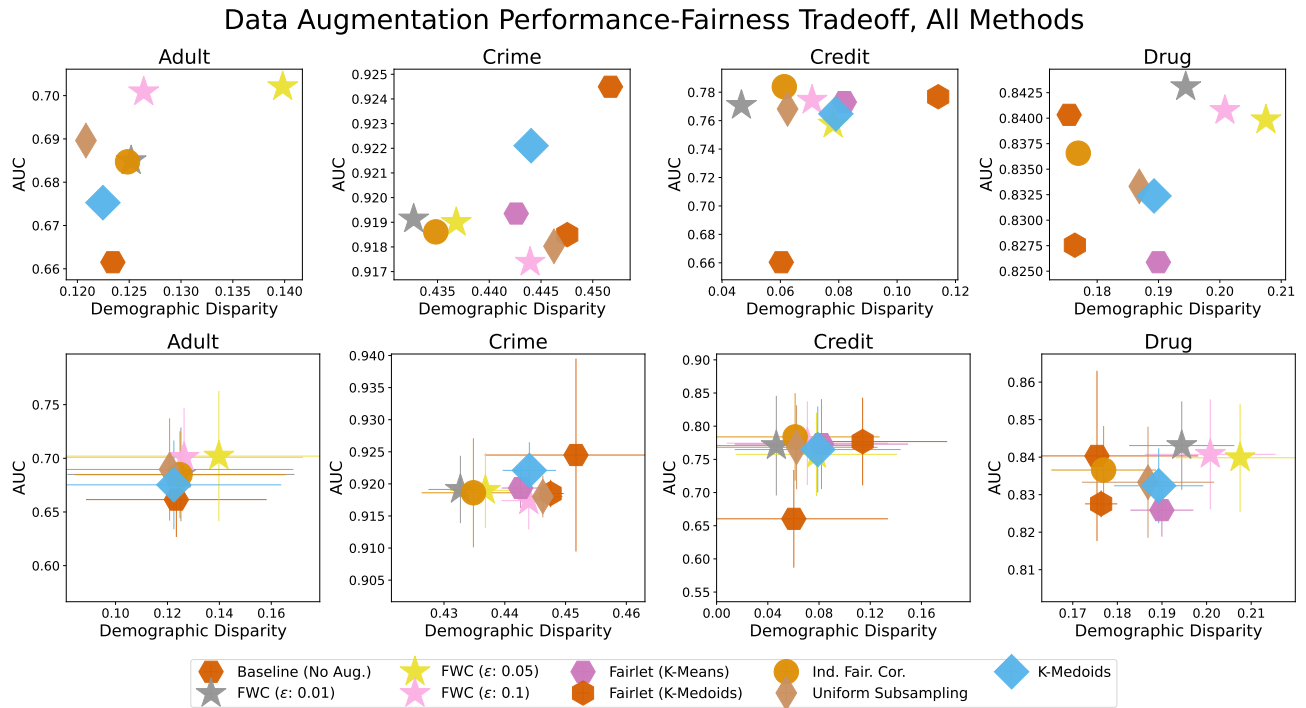


Figure 6. Fairness-utility tradeoff of downstream MLP classifier trained using the original training set augmented with coresets representative, following the augmentation strategy from Sharma et al. (2020), including all methods mentioned in Section 5. Each point shows the best model in terms of performance-fairness tradeoff over various degrees of data augmentation, in addition to the baseline model with no augmentation. Averages and standard deviations computed over 10 runs, with the top panel showing just means and the bottom panel combining both means and standard deviations.

Using FWC coresets to correct biases in LLMs To query GPT models, test data with 200 samples is provided with a base parity of 0.5 (similar to Wang et al. (2023)) and additionally, examples are provided in the case of the few shot settings. Data is fed in as text. One of the tabular data, for example, is: “A person in 1996 has the following attributes: Age: 21.0, workclass: Private, education: Some-college, highest education level: 10.0, marital status: Never-married, occupation: Other-service, relationship: Own-child, race: White, sex: Female, capital gain: 0.0, capital loss: 0.0, hours per week: 25.0, native country: United-States”.

We use the following prompts:

- **Zero shot:** “Using the provided data, will this person from 1996 be hired at greater than 50,000 USD per year? You must only respond with the word ‘yes’ or ‘no’. Here are 0 examples with the correct answer.”
- **Few shot:** “Given the provided data, will this person from 1996 be hired at greater than 50,000 USD per year? You must only respond with the word ‘yes’ or ‘no’. Here are n examples with the correct income level for a person in 1996. Make sure you use the examples as a reference”, where n is the number of demographically balanced samples.
- **Few shot (FWC):** “Given the provided data, will this from 1996 be hired at greater than 50,000 USD per year? You must only respond with the word ‘yes’ or ‘no’. Here are n examples with the correct income level for a person in 1996, along with weights in the column weight. Weights are between 0 (minimum) and 1 (maximum). The more the weight, the more important the example is. Make sure you use the examples as a reference.”

In the few shot settings, 16 examples are provided in both cases due to the LLM token limitation; passing fewer examples yields similar results to the ones in Table 2. For FWC, we run a separate coreset generation run (differently from other experiments in Section 5), where we selected $m = 16$ and we ensured that the positive class ($Y = 1$) has an equal number of male and female samples. We also note that while the results from GPT-4 for the zero shot and few shot cases are similar to what was observed by Wang et al. (2023), the accuracies reported for the GPT-3.5 Turbo model appear to be lower in our experiments, which points to a potential difference in the exact backend LLM model used for inference.

Fairness-utility tradeoff when using coresets for training downstream models Figure 7 expands the results provided in Figure 1 and shows all the fairness-utility tradeoffs for all methods across the four datasets, both with (right column) and without (left column) using a pre-processing fairness approach (Kamiran & Calders, 2012) (excluding FWC, to which no fairness modification is applied after coresets have been generated). For each method, the coreset size which achieves the best fairness-utility tradeoff is shown (which is not necessarily the coreset with the largest size). FWC achieves a competitive fairness-utility tradeoff with respect to other competing methods, when using the generated coresets to train a downstream MLP classifier model. FWC consistently reduces disparity in the downstream classification with respect to other approaches, and often maintaining the same utility (indicated by the AUC). For completeness, Figure 8 also reports standard deviations for the fairness-utility tradeoff; standard deviations for the Adult and Credit datasets are large due to the MLP classifier becoming trivial (i.e., always returning 0s or 1s), which yields very low performance but has no demographic disparity (by definition, as all test samples are assigned the same outcome).

Fair Coresets via Optimal Transport

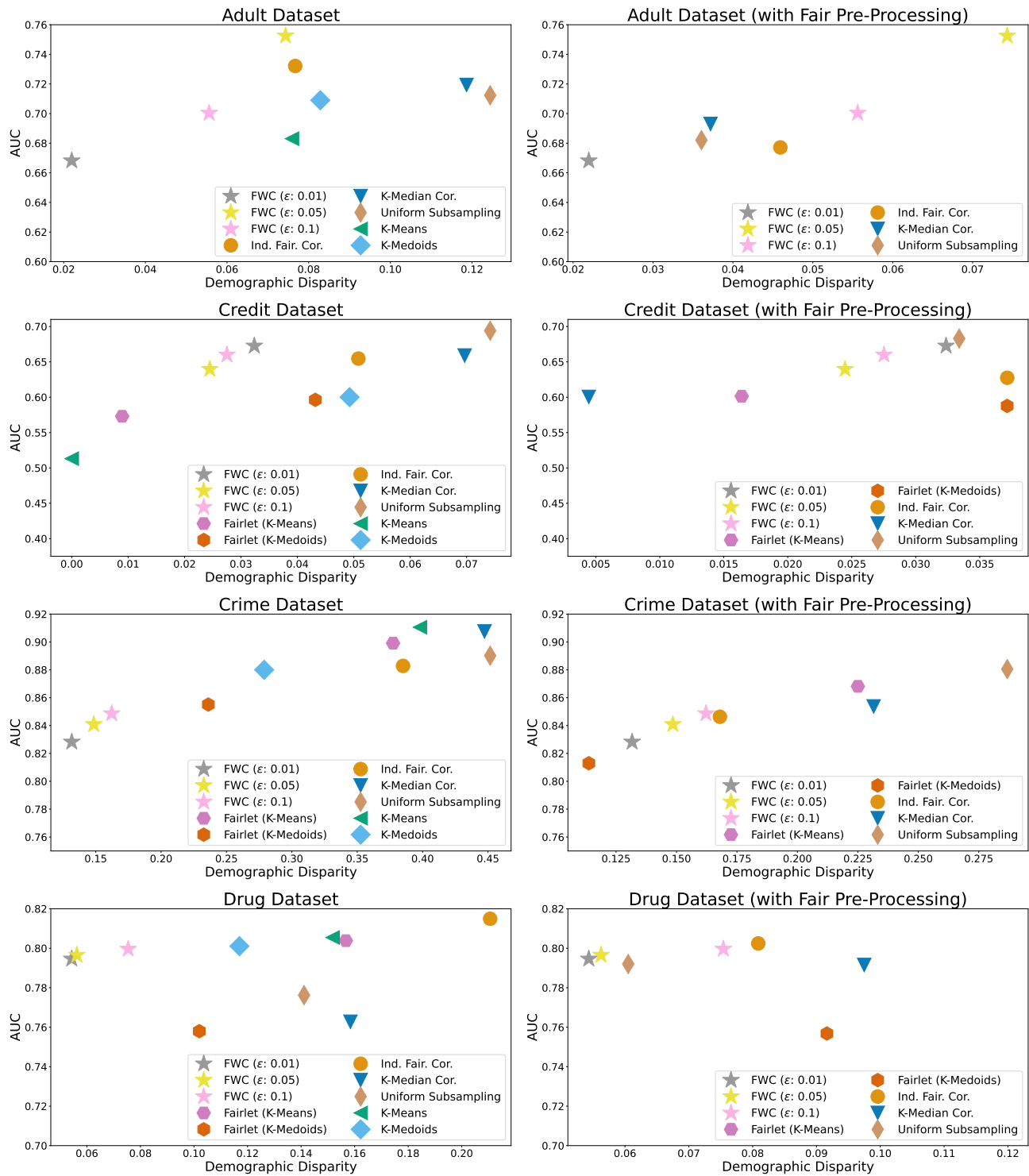


Figure 7. Fairness-utility tradeoff of all methods, indicated by AUC and demographic disparity of a downstream MLP classifier across all datasets (rows) and without (left column) or with (right column) fair pre-processing (Kamiran & Calders, 2012) (excluding FWC, to which no fairness modification is applied after coresets have been generated). We report the averages over 10 separate train/test splits.

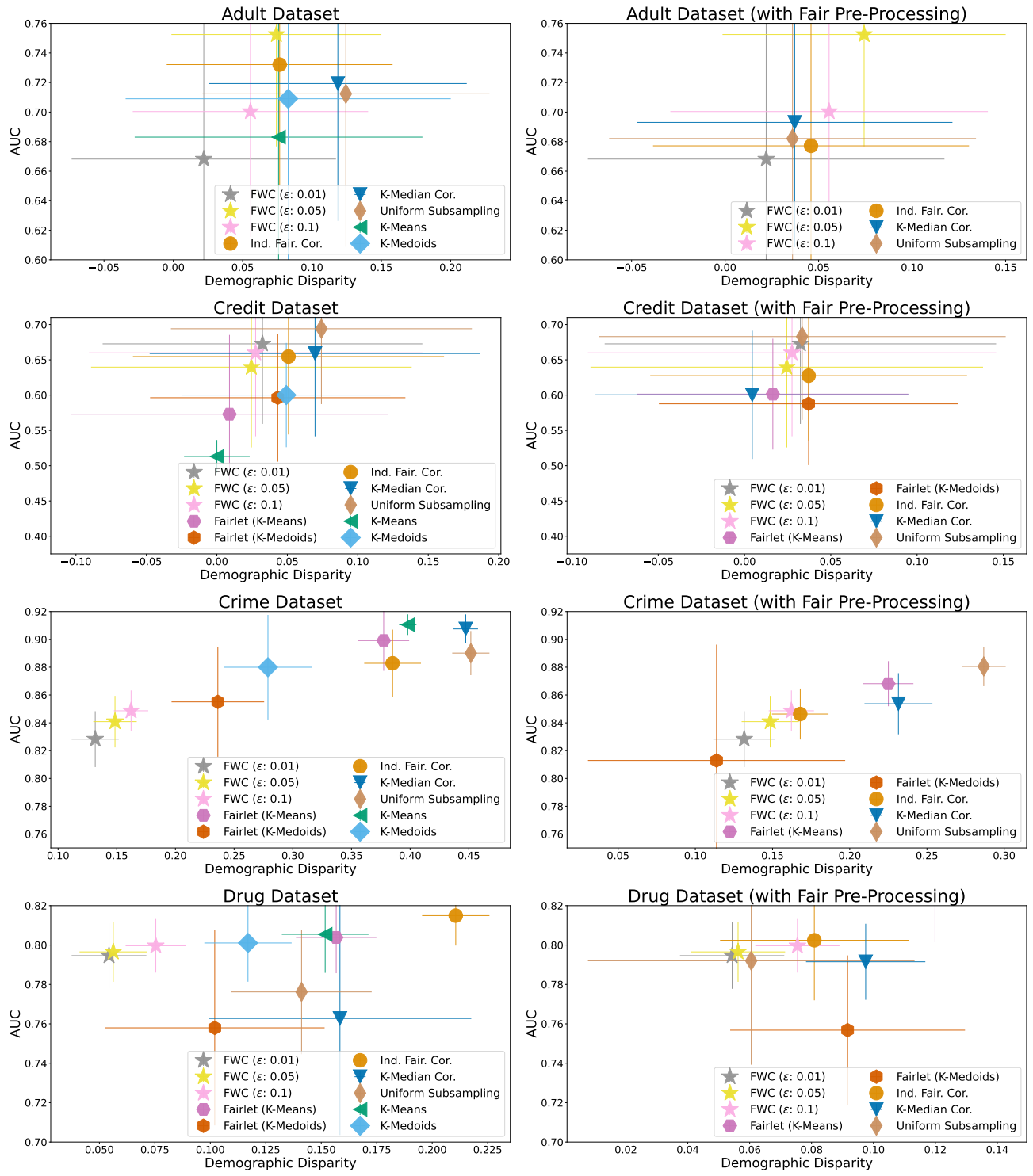


Figure 8. Similarly to Figure 7, we report the means and standard deviations over 10 runs of the fairness-utility tradeoff of all methods, indicated by AUC and demographic disparity of a downstream MLP classifier across all datasets (rows) and without (left column) or with (right column) fair pre-processing (Kamiran & Calders, 2012) (excluding FWC, to which no fairness modification is applied after coresets have been generated).